THE ASTROPHYSICAL JOURNAL SUPPLEMENT SERIES, 95:345–369, 1994 December

THE SECOND CALTECH–JODRELL BANK VLBI SURVEY. I. OBSERVATIONS OF 91 OF 193 SOURCES

G. B. TAYLOR, R. C. VERMEULEN, T. J. PEARSON, AND A. C. S. READHEAD
California Institute of Technology, Owens Valley Radio Observatory, 105-24, Pasadena, CA 91125

AND

D. R. HENSTOCK, I. W. A. BROWNE, AND P. N. WILKINSON
University of Manchester, Nuffield Radio Astronomy Laboratories, Jodrell Bank, Macclesfield, Cheshire SK11 9DL, UK
Received 1994 April 26; accepted 1994 May 20

ABSTRACT

We define the sample for the second Caltech–Jodrell Bank VLBI survey. This is a sample of 193 flat- or gigahertz-peaked-spectrum sources selected at 4850 MHz. This paper presents images of 91 sources with a resolution of ~1 mas, obtained using VLBI observations at 4992 MHz with a global array. The remaining images and the integrated radio spectra will be presented in a forthcoming paper by Henstock et al.

Subject headings: galaxies: structure — quasars: general — radio continuum: galaxies — surveys — techniques: interferometric

1. INTRODUCTION

The second Caltech–Jodrell Bank VLBI survey (CJ2) is a Mark II snapshot VLBI survey of 193 flat- and peaked-spectrum radio sources. The survey extends the morphological study of the Pearson & Readhead (1988, hereafter PR) and the first Caltech–Jodrell Bank (Polatidis et al. 1994; Thakkar et al. 1994; Xu 1994; hereafter CJ1) surveys to 321 sources. With uniform observations of a large sample, it is possible to pursue classification and evolutionary issues in detail and to test unification schemes. The CJ2 survey also has three cosmological goals: (1) to search for small-separation gravitationally lensed systems and hence to look directly for mass concentrations in the unexplored range of 10^6–10^9 $M_\odot$, (2) to populate the proper motion–redshift diagram for superluminal sources, and (3) to populate the angular size–redshift diagram for compact sources (both diagrams can be used to estimate the deceleration parameter, q_0).

In this paper we define the CJ2 sample and report on the first three observing campaigns, during which 91 sources were observed and imaged. Results for the remainder of the sample and plots of the integrated radio spectra for the entire sample are presented in Henstock et al. (1994, hereafter Paper II). In § 2 we discuss how the source sample was derived. A brief description of the observations is presented in § 3, and the images are presented in § 4. Future work will concentrate on the morphological classification (Taylor et al. 1994) and the constraints which these observations place on gravitational lensing by objects in the mass range of 10^6–10^9 $M_\odot$ (Henstock 1994). A campaign to obtain redshifts and improved optical identifications for the CJ2 sample is underway.

2. THE CJ2 SAMPLE SELECTION

The CJ2 sample is drawn from the Jodrell Bank–VLA Astrometric Survey (Patnaik et al. 1992, and papers in preparation; hereafter JVAS), which contains ~920 compact flat-spectrum sources north of declination 35°. The primary goal of that survey was to identify strong, compact sources at 8400 MHz and to measure their positions accurately enough for use as phase calibrators for the Jodrell Bank MERLIN. For declinations between 35° and 75°, sources in the JVAS catalog were derived from the 1400 and 4850 MHz Green Bank surveys (Condon & Broderick 1985, 1986; Condon, Broderick, & Seielstad 1989; Gregory & Condon 1991). Sources north of declination 75° were selected from the MPI S5 catalog (Kühr et al. 1981). The JVAS sources were selected with spectral indices between 1400 and 4850 MHz flatter than $\alpha = -0.5$ (where $S_\nu \propto \nu^\alpha$). The vast majority of the JVAS sources are unresolved by the ~200 mas VLA beam at 8400 MHz.

The selection criteria for the CJ2 sample were:

1. Observed in JVAS;
2. Flux density at 4850 MHz (Gregory & Condon 1991), $S_{4850} \geq 350$ mJy;
3. Declination (B1950) $\delta \geq 35°$;
4. Galactic latitude $|b| \geq 10°$;
5. Spectral index (α^{365}_{8400} flatter than -0.5);
6. Not previously observed in the PR or CJ1 surveys.

To increase the sample size of CJ2 in the search for small-scale gravitational lenses, we also included 11 sources weaker than 350 mJy at 4850 MHz, 4 sources with α^{365}_{8400} steeper than -0.5, and one source, 0026 + 346, just below our declination limit. A similar number of flat-spectrum sources stronger than 350 mJy were not observed because of missing information at lower frequencies, or because they were not included in JVAS. By selecting the CJ2 sample from the observed JVAS sample, rather than from the Green Bank catalog, we made use of better source positions and increased the likelihood of observing sources with compact structure on the milliarcsecond scale. Since flat-spectrum sources are known to be more compact than steep-spectrum sources, we excluded sources with evidence for a steep spectrum ($\alpha < -0.5$) between 365 MHz (J. Douglas, private communication) and 8400 MHz (JVAS). The net result of our selection procedure is not a complete, flux and spectrally limited sample. A complete sample of sources imaged with VLBI and suitable for statistical studies will be formed using the PR, CJ1, and CJ2 surveys and discussed in a later paper.

Positions, flux densities, and optical identifications for all 193 sources in the CJ2 sample are listed in Table 1. Spectra for all sources are presented in Paper II. The optical identifications and estimates of the apparent magnitudes were made with the aid of the Automatic Plate Measuring Facility at the Institute of Astronomy, Cambridge, which was used to scan the POSS plates around the JVAS positions (McMahon 1994).

3. OBSERVATIONS

The observations took place on 1992 June 5–7, 1992 September 24–27, and 1993 March 1–2 using a global VLBI array. Results from a further observing session on 1993 June 9–16 will be presented in Paper II. The telescopes used include those in the European VLBI Network, the Very Long Baseline Array,[1] the Very Large Array,[1] the NRAO 140 foot (43 m),[1] and the Haystack Observatory. The observing frequency was 4992 MHz, and the Mark II recording scheme was used, providing a bandwidth of 2 MHz. Only the signals from telescopes successfully observing in left-circular polarization were used. These telescopes are listed for each observing session in Table 2.

The observing strategy employed was a "VLBI-snapshot" technique, in which each source was observed in three, or sometimes four, scans each of 20 minutes duration distributed over a wide hour-angle range. The typical *u*-*v* coverages obtained for sources at high, middle, and low declinations are shown in Figure 1. A more detailed discussion of the VLBI-snapshot technique may be found in Polatidis et al. (1994).

All data were correlated using the Block II Correlator at Caltech. Observations of strong calibrators, primarily 0552 + 398 and 1739 + 522, were used to find and monitor the clock offsets at intervals of ~12 hr during each run. Following correlation, global fringe fitting was performed using the AIPS task FRING, an implementation of the Schwab & Cotton (1983) algorithm. A solution interval of ~7 minutes was used allowing for three solutions of the delay and fringe rate during each 20 minute scan. The fringe fitting was performed using the least-squares option within FRING and assuming a point source model in all cases. Effelsberg was chosen to be the "reference telescope" whenever possible, otherwise the NRAO 140 foot telescope at Green Bank was used.

Amplitude calibration for each antenna was derived from measurements of the antenna gain and system temperature during the run. In addition the calibrators 0552 + 398 and 1739 + 522 were observed throughout the run to further refine the amplitude calibration by examining *u*-*v* crossing points as described by Polatidis et al. (1994). After phase self-calibration with a 10 s solution interval, and a point-source model, the data were coherently averaged to 1 minute integrations. All editing, imaging, deconvolution, and self-calibration of the data were performed using DIFMAP (Shepherd, Pearson, &

[1] The National Radio Astronomy Observatory is operated by Associated Universities, Inc., under cooperative agreement with the National Science Foundation.

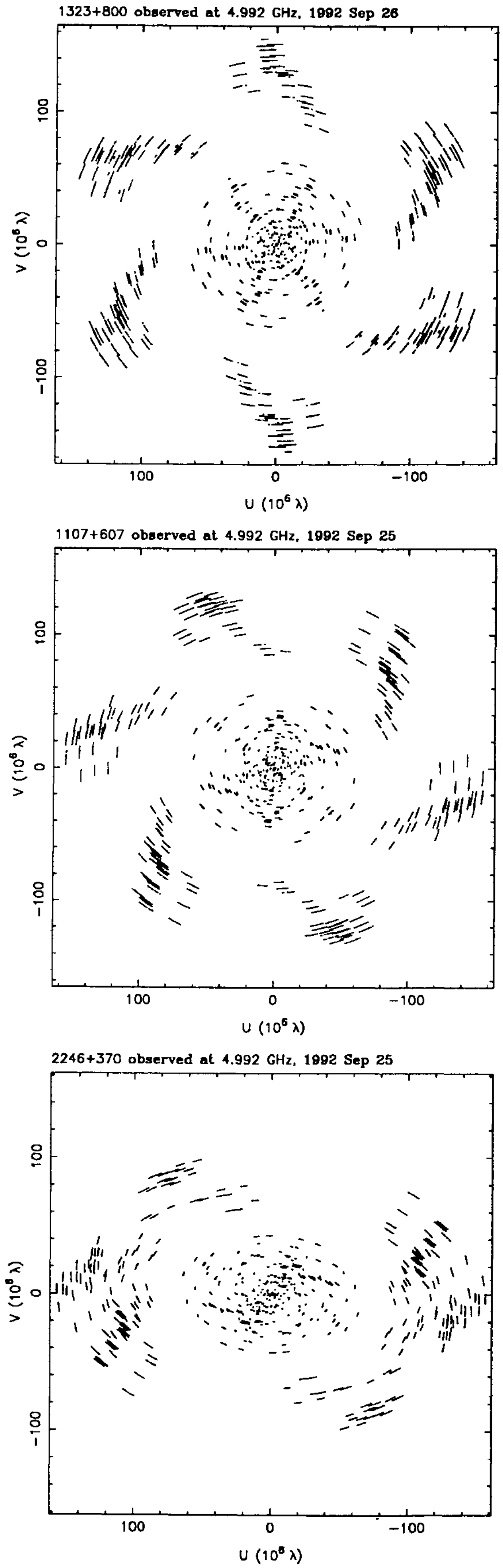

FIG. 1.—*u*-*v* coverage obtained for three sources at declinations of 80°, 60°, and 37°. The hexagonal pattern results from the three observations of 20 minutes each spaced over a wide range in hour angle.

TABLE 1

THE CJ2 SAMPLE

Source (1)	R.A. (2)	Declination (3)	S_{80cm} (4)	S_{20cm} (5)	S_{6cm} (6)	$S_{3.6cm}$ (7)	ID (8)	R (9)	z (10)	Date (11)
0003+380 ...	00 05 57.17550	38 20 15.1685	0.638	0.601	0.549	1.157	G	17.1	0.229	1993 Jun
0014+813 ...	00 17 08.47504	81 35 08.1365	–	0.676	0.551	1.355	Q	15.9[a]	3.384	1992 Sep
0018+729 ...	00 21 27.37784	73 12 41.9283	–	0.614	0.397	0.196	EF	–	...	1992 Jun
0026+346 ...	00 29 14.24355	34 56 32.2545	1.359	1.750	1.312	1.035	EF	–	...	1992 Jun
0035+413 ...	00 38 24.84498	41 37 06.0046	0.512	0.440	1.114	0.985	Q	19.4	1.353	1993 Jun
0109+351 ...	01 12 12.94503	35 22 19.2954	0.915	0.360	0.362	0.402	BS	17.8	...	1993 Jun
0110+495 ...	01 13 27.00695	49 48 24.0572	1.104	0.486	0.710	0.499	Q	17.5[b]	0.395	1993 Jun
0129+431 ...	01 32 44.12727	43 25 32.6667	–	0.216	0.347	0.235	BS	18.7	...	1993 Jun
0145+386 ...	01 48 24.37679	38 54 05.2227	0.209	0.293	0.370	0.343	Q	17.2	1.44	1993 Jun
0151+474 ...	01 54 56.29019	47 43 26.5392	0.384	0.353	0.505	0.690	EF	–	...	1993 Jun
0201+365 ...	02 04 55.59586	36 49 18.0007	0.460	0.590	0.349	0.263	Q	17.5	2.912	1993 Jun
0205+722 ...	02 09 51.79208	72 29 26.6686	–	0.842	0.560	0.549	RO	17.0[b]	...	1992 Sep
0227+403 ...	02 30 45.70679	40 32 53.0870	0.252	0.438	0.436	0.578	BS	17.0[b]	...	1993 Jun
0249+383 ...	02 53 08.88698	38 35 24.9867	0.970	0.781	0.450	0.454	BS	18.5	...	1993 Jun
0251+393 ...	02 54 42.63160	39 31 34.7140	–	0.297	0.408	0.367	BS	15.4	...	1993 Jun
0256+424 ...	02 59 38.38223	42 36 43.1192	0.685	0.616	0.366	0.320	EF	–	...	1993 Jun
0307+380 ...	03 10 49.88050	38 14 53.8452	–	–	0.760	0.453	EF	–	...	1993 Jun
0309+411 ...	03 13 01.96146	41 20 01.1903	0.474	0.467	0.516	0.673	G	16.0[b]	0.136	1993 Jun
0340+362 ...	03 43 28.95271	36 22 12.4404	0.454	0.282	0.376	0.620	EF	–[b]	...	1993 Jun
0346+800 ...	03 54 46.12577	80 09 28.8156	–	–	0.396	0.365	BO	21.3	...	1992 Sep
0444+634 ...	04 49 23.30971	63 32 09.4532	0.535	0.370	0.606	0.467	Q	19.0[b]	0.781	1992 Sep
0537+531 ...	05 41 16.17329	53 12 24.8379	1.115	0.656	0.665	0.747	Q	17.4[a]	1.275	1993 Mar
0546+726 ...	05 52 52.99716	72 40 45.1288	–	0.493	0.401	0.267	NS	17.0[b]	...	1992 Sep
0554+580 ...	05 59 13.39407	58 04 03.4432	0.630	0.373	0.906	0.501	BS	18.0[b]	...	1993 Mar
0600+442 ...	06 04 35.62972	44 13 58.5460	1.486	1.208	0.705	0.439	BS	17.0[b]	...	1993 Jun
0604+728 ...	06 10 48.86913	72 48 53.1885	–	1.015	0.654	0.391	EF	–	...	1992 Sep
0609+607 ...	06 14 23.86660	60 46 21.7540	1.562	1.060	1.059	0.750	BS	19.0[b]	...	1993 Mar
0627+532 ...	06 31 34.68599	53 11 27.7537	0.605	0.807	0.485	0.312	BS	18.5	...	1993 Jun
0633+734 ...	06 39 21.96228	73 24 58.0503	–	1.097	0.748	0.772	BS	17.8	...	1992 Sep
0633+596 ...	06 38 02.87300	59 33 22.2075	0.295	0.230	0.482	0.553	EF	–	...	1993 Mar
0636+680 ...	06 42 04.25682	67 58 35.6258	–	0.129	0.499	0.436	Q	16.2	3.174	1992 Jun
0641+393 ...	06 44 53.71000	39 14 47.5407	0.529	0.366	0.453	0.616	BS	19.5[b]	...	1993 Jun
0650+453 ...	06 54 23.71370	45 14 23.5410	0.466	0.590	0.420	0.372	BO	21.0	...	1993 Jun
0651+410 ...	06 55 10.02429	41 00 10.1479	–	–	0.425	0.373	G	14.0[b]	0.0201	1993 Jun
0700+470 ...	07 04 09.55875	47 00 56.0405	0.558	0.824	0.443	0.335	RO	20.0	...	1993 Jun
0702+612 ...	07 07 00.61645	61 10 11.5875	0.610	0.327	0.370	0.235	BS	17.0	...	1993 Mar
0714+457 ...	07 17 51.85314	45 38 03.2521	–	0.408	0.480	0.569	Q	17.7	0.940	1993 Jun
0718+793 ...	07 26 11.74592	79 11 31.0208	–	0.463	0.631	0.694	EF	–	...	1992 Sep
0724+571 ...	07 28 49.63210	57 01 24.3667	0.552	0.408	0.393	0.632	BS	17.0[b]	...	1993 Mar
0727+409 ...	07 30 51.34725	40 49 50.8263	0.242	0.413	0.468	0.377	Q	17.0[b]	2.501	1993 Jun
0730+504 ...	07 33 52.52117	50 22 09.0511	0.761	0.386	0.890	0.730	BS	19.0[b]	...	1992 Jun
0731+479 ...	07 35 02.31207	47 50 08.4202	0.351	0.432	0.533	0.450	Q	16.9	0.782	1993 Jun
0733+597 ...	07 37 30.08713	59 41 03.1948	0.862	0.553	0.357	0.235	G	14.9[c]	0.040	1993 Mar
0738+491 ...	07 42 02.75080	49 00 15.6021	–	–	0.352	0.483	EF	–	...	1993 Jun
0739+398 ...	07 43 09.88664	39 41 30.7813	1.286	0.770	0.410	0.327	Q	18.0	1.700	1993 Jun
0740+768 ...	07 47 14.62258	76 39 17.2644	–	–	0.592	0.550	EF	–	...	1992 Sep
0743+744 ...	07 49 22.45732	74 20 41.5949	–	0.354	0.479	0.394	Q	18.8	1.629	1993 Jun
0749+540 ...	07 53 01.38500	53 52 59.6370	–	0.791	0.877	1.162	BL	17.3	–	1993 Mar
0749+426 ...	07 53 03.33778	42 31 30.7631	0.760	0.702	0.461	0.280	RS	18.1	...	1992 Jun
0803+452 ...	08 06 33.47197	45 04 32.2740	0.272	0.389	0.414	0.423	BS	19.6	...	1993 Jun
0806+573 ...	08 11 00.60937	57 14 12.4939	0.927	–	0.405	0.348	BS	17.2	...	1992 Jun
0821+621 ...	08 25 38.61209	61 57 28.5773	1.066	0.652	0.615	0.608	Q	17.3	0.542	1992 Jun
0824+355 ...	08 27 38.58906	35 25 05.0807	1.832	0.866	0.746	0.657	Q	19.7	2.249	1993 Jun
0830+425 ...	08 33 53.88502	42 24 01.8494	0.405	–	0.341	0.553	NS	17.0	...	1993 Jun
0833+416 ...	08 36 36.89322	41 25 54.7062	0.473	0.425	0.385	0.279	BS	17.2	...	1993 Jun

TABLE 1—*Continued*

Source (1)	R.A. (2)	Declination (3)	S_{80cm} (4)	S_{20cm} (5)	S_{6cm} (6)	$S_{3.6cm}$ (7)	ID (8)	R (9)	z (10)	Date (11)
0843+575 ...	08 47 28.06159	57 23 38.3355	–	0.284	0.384	0.242	EF	–	...	1993 Mar
0859+681 ...	09 03 53.15590	67 57 22.6827	0.413	0.592	0.751	0.635	Q	18.2	1.499	1992 Jun
0900+520 ...	09 03 58.57582	51 51 00.6583	–	0.322	0.395	0.273	BS	19.6	...	1993 Mar
0902+490 ...	09 05 27.46476	48 50 49.9588	0.976	0.636	0.547	0.447	Q	17.2	2.690	1993 Jun
0913+391 ...	09 16 48.90469	38 54 28.1421	1.801	1.057	0.557	0.462	Q	19.0[b]	1.269	1993 Jun
0925+504 ...	09 29 15.44170	50 13 35.9782	–	0.266	0.558	0.692	BS	16.0	...	1993 Jun
0927+352 ...	09 30 55.27914	35 03 37.6082	1.053	0.422	0.383	0.472	NS	19.2	...	1993 Jun
0929+533 ...	09 32 41.15174	53 06 33.7851	0.483	0.537	0.384	0.380	Q	17.4	0.595	1993 Mar
0930+493 ...	09 34 15.76310	49 08 21.7164	0.488	0.733	0.574	0.398	BS	18.4	...	1993 Jun
0933+503 ...	09 37 12.32879	50 08 52.0753	–	–	0.347	0.352	G	18.0	...	1993 Jun
0941+522 ...	09 44 52.15670	52 02 34.2164	0.906	0.851	0.345	0.258	Q	17.8[b]	0.565	1993 Jun
0942+468 ...	09 45 42.09361	46 36 50.5928	0.403	0.278	0.354	0.356	EF	–	...	1993 Jun
0949+354 ...	09 52 32.02616	35 12 52.3929	0.510	0.344	0.403	0.337	Q	18.9	1.875	1993 Jun
0950+748 ...	09 54 47.44405	74 35 57.1405	–	1.186	0.738	0.411	EF	–	...	1992 Sep
1010+350 ...	10 13 49.61423	34 45 50.7817	0.469	0.418	0.597	0.367	G	18.6	1.414	1993 Jun
1014+615 ...	10 17 25.88496	61 16 27.4932	0.265	0.361	0.631	0.571	BS	18.1	...	1992 Sep
1030+398 ...	10 33 22.06179	39 35 51.0812	0.823	0.379	0.645	0.509	EF	–	...	1993 Jun
1030+611 ...	10 33 51.42726	60 51 07.3301	0.995	0.766	0.579	0.427	NS	19.3	0.336	1992 Sep
1038+528 ...	10 41 46.77999	52 33 28.2170	1.121	0.713	0.709	0.720	Q	16.3	0.677	1993 Jun
1041+536 ...	10 44 10.67165	53 22 20.5222	0.493	0.543	0.481	0.389	BS	19.0	...	1993 Jun
1058+629 ...	11 01 53.44908	62 41 50.5899	1.882	0.598	0.700	0.354	BS	17.7	...	1992 Sep
1105+437 ...	11 08 23.47791	43 30 53.6367	0.357	0.266	0.375	0.282	NS	19.5	...	1993 Jun
1107+607 ...	11 10 13.08711	60 28 42.5510	0.439	0.345	0.404	0.276	EF	–	...	1992 Sep
1124+455 ...	11 26 57.65509	45 16 06.2894	–	0.493	0.355	0.333	BS	17.0	...	1993 Jun
1124+571 ...	11 27 40.13530	56 50 14.7793	0.427	0.775	0.597	0.498	Q	18.0	2.890	1992 Sep
1125+596 ...	11 28 13.34150	59 25 14.7776	0.279	0.364	0.393	0.584	BS	20.0	...	1992 Sep
1143+590 ...	11 46 26.91199	58 48 34.2423	–	0.276	0.674	0.569	BS	19.6	...	1992 Sep
1144+352 ...	11 47 22.13022	35 01 07.5258	0.358	0.695	0.663	0.501	G	15.0	0.063	1993 Jun
1146+531 ...	11 48 56.56863	52 54 25.3311	–	–	0.304	0.597	BS	15.5	...	1993 Jun
1146+596 ...	11 48 50.35909	59 24 56.3620	0.327	0.415	0.627	0.516	G	11.0	0.0108	1992 Sep
1151+408 ...	11 53 54.65938	40 36 52.6172	0.949	0.698	0.380	0.361	NS	19.5	...	1993 Jun
1155+486 ...	11 58 26.76904	48 25 16.2350	0.309	0.484	0.445	0.424	BO	19.9	...	1993 Jun
1205+544 ...	12 08 27.49949	54 13 19.5292	–	0.463	0.397	0.280	EF	–	...	1993 Jun
1206+415 ...	12 09 22.78840	41 19 41.3688	–	0.323	0.515	0.486	BS	16.3	...	1993 Jun
1214+588 ...	12 17 11.02025	58 35 26.2283	0.710	0.422	0.307	0.473	BS	19.5	...	1992 Sep
1218+444 ...	12 21 27.04576	44 11 29.6635	0.662	0.601	0.478	0.435	BS	17.3	...	1992 Jun
1221+809 ...	12 23 40.49739	80 40 04.3239	–	0.726	0.518	0.454	BL	18.7	–	1993 Jun
1223+395 ...	12 25 50.57029	39 14 22.6806	0.544	0.540	0.438	0.377	EF	–	...	1993 Jun
1226+373 ...	12 28 47.42456	37 06 12.0820	0.263	0.192	0.953	0.868	BS	18.0[b]	...	1993 Jun
1239+376 ...	12 42 09.81383	37 20 05.6807	0.469	0.544	0.446	0.336	EF	–	...	1993 Jun
1240+381 ...	12 42 51.37049	37 51 00.0126	0.495	0.363	0.768	0.608	Q	19.1	1.316	1993 Jun
1246+586 ...	12 48 18.78472	58 20 28.7144	0.232	0.238	0.414	0.310	BS	14.0	...	1992 Sep
1250+532 ...	12 53 11.92132	53 01 11.7266	0.982	0.538	0.396	0.372	BS	16.4	...	1993 Jun
1254+571 ...	12 56 14.23440	56 52 25.2367	0.551	0.288	0.419	0.255	G	13.2[b]	0.041	1992 Sep
1258+507 ...	13 00 41.24832	50 29 36.7498	0.666	0.524	0.391	0.339	EF	–	...	1993 Jun
1300+580 ...	13 02 52.46490	57 48 37.6175	0.403	0.305	0.758	0.885	RO	20.0[b]	...	1992 Sep
1307+562 ...	13 09 09.75329	55 57 38.1932	0.319	0.294	0.416	0.302	BS	17.6	...	1992 Sep
1308+471 ...	13 10 53.59063	46 53 52.2192	–	–	0.393	0.361	BS	19.1	...	1993 Jun
1309+555 ...	13 11 03.20969	55 13 54.3298	0.595	0.207	0.677	0.505	BS	19.1	...	1992 Sep
1311+552 ...	13 13 37.85179	54 58 23.8943	1.645	1.173	0.542	0.302	EF	–	...	1992 Sep
1312+533 ...	13 14 43.82839	53 06 27.7274	–	0.232	0.433	0.303	EF	–	...	1993 Jun
1321+410 ...	13 24 12.09400	40 48 11.7728	–	0.357	0.413	0.246	NS	19.5	...	1993 Jun
1322+835 ...	13 21 45.59214	83 16 13.4365	–	–	0.506	0.267	EF	–	...	1992 Sep
1323+800 ...	13 23 51.57398	79 42 51.8592	–	0.492	0.458	0.564	EF	–	...	1992 Sep
1325+436 ...	13 27 20.97896	43 26 27.9969	0.660	0.703	0.533	0.462	Q	18.5	2.073	1993 Jun

TABLE 1—*Continued*

Source (1)	R.A. (2)	Declination (3)	S_{80cm} (4)	S_{20cm} (5)	S_{6cm} (6)	$S_{3.6cm}$ (7)	ID (8)	R (9)	z (10)	Date (11)
1335+552 ...	13 37 49.64084	55 01 02.1208	0.744	0.717	0.811	0.573	Q	17.8	1.096	1992 Sep
1337+637 ...	13 39 23.78121	63 28 58.4253	–	0.500	0.431	0.272	BS	18.5	...	1992 Sep
1342+662 ...	13 43 45.95763	66 02 25.7486	–	–	0.288	0.578	Q	18.8	0.766	1992 Jun
1413+373 ...	14 15 28.46657	37 06 21.1789	0.213	0.366	0.383	0.278	Q	17.3	2.36	1993 Jun
1415+463 ...	14 17 08.16081	46 07 05.4483	1.525	1.012	0.904	0.583	Q	17.5	1.552	1993 Jun
1417+385 ...	14 19 46.61407	38 21 48.4841	0.487	0.708	0.871	0.793	Q	18.5	1.832	1993 Jun
1421+482 ...	14 23 06.15619	48 02 10.8466	0.497	0.361	0.536	0.392	BS	18.9	...	1993 Jun
1424+366 ...	14 26 37.08764	36 25 09.5858	0.336	0.194	0.429	0.621	BS	18.3	...	1993 Jun
1427+543 ...	14 29 21.87958	54 06 11.1266	2.375	0.903	0.718	0.493	BS	20.7	...	1993 Jun
1436+763 ...	14 35 47.09760	76 05 25.8179	–	1.154	0.585	0.417	EF	–	...	1992 Sep
1442+637 ...	14 43 58.60200	63 32 26.3630	0.388	0.684	0.456	0.392	Q	17.3	1.380	1992 Jun
1448+762 ...	14 48 28.77822	76 01 11.5943	–	0.513	0.683	0.324	EF	–	...	1993 Jun
1456+375 ...	14 58 44.79492	37 20 21.6266	–	0.335	0.591	0.370	NS	18.2	...	1993 Jun
1459+480 ...	15 00 48.65431	47 51 15.5259	0.432	0.401	0.489	0.686	BS	17.1	...	1993 Jun
1505+428 ...	15 06 53.04195	42 39 23.0400	0.456	0.435	0.404	0.410	BS	21.5	...	1993 Jun
1526+670 ...	15 26 42.87323	66 50 54.6171	–	0.426	0.417	0.312	NS	17.1	...	1992 Sep
1531+722 ...	15 31 33.57679	72 06 41.2196	–	0.661	0.452	0.231	Q	16.5[b]	0.899	1992 Sep
1534+501 ...	15 35 52.03949	49 57 39.0837	–	0.229	0.359	0.312	BS	18.0	...	1993 Jun
1543+480 ...	15 45 08.53027	47 51 54.6667	0.835	0.665	0.441	0.347	EF	–	...	1993 Jun
1543+517 ...	15 45 02.82440	51 35 00.8780	0.614	0.485	0.544	0.629	BS	17.3	...	1993 Jun
1545+497 ...	15 47 21.13841	49 37 05.8100	1.690	0.936	0.549	0.360	RS	19.6	...	1993 Jun
1550+582 ...	15 51 58.20771	58 06 44.4659	–	0.226	0.367	0.305	BS	17.0[b]	...	1993 Jun
1602+576 ...	16 03 55.93111	57 30 54.4146	–	–	0.351	0.312	Q	16.8	2.858	1993 Jun
1619+491 ...	16 20 31.22632	49 01 53.2537	0.619	0.468	0.469	0.386	BS	17.8	...	1993 Jun
1623+569 ...	16 24 32.17968	56 52 28.0063	–	0.213	0.213	0.371	BS	17.0	...	1993 Mar
1629+495 ...	16 31 16.54118	49 27 39.5032	0.693	0.323	0.394	0.626	RS	18.3	...	1993 Jun
1636+473 ...	16 37 45.13069	47 17 33.8364	2.062	0.949	1.330	0.749	Q	17.0	0.740	1993 Jun
1638+540 ...	16 39 39.84349	53 57 47.1166	–	0.310	0.369	0.298	BS	19.7	...	1993 Jun
1645+410 ...	16 46 56.85906	40 59 17.1742	–	0.315	0.388	0.358	BS	20.6	...	1993 Jun
1645+635 ...	16 45 58.55338	63 30 10.9322	0.420	0.298	0.444	0.214	BS	19.4	...	1992 Sep
1656+571 ...	16 57 20.70951	57 05 53.5053	2.425	0.806	0.844	0.533	Q	16.8	1.290	1992 Sep
1700+685 ...	17 00 09.29376	68 30 06.9590	0.619	0.300	0.435	0.377	G	17.0	...	1992 Sep
1716+686 ...	17 16 13.93808	68 36 38.7403	–	0.412	0.988	0.829	Q	17.0	0.777	1992 Jun
1722+401 ...	17 24 05.42882	40 04 36.4605	1.040	0.551	0.532	0.284	BS	21.7	...	1993 Jun
1726+455 ...	17 27 27.65082	45 30 39.7339	0.654	0.425	1.066	1.331	Q	18.0[b]	0.714	1993 Jun
1734+363 ...	17 35 48.08683	36 16 45.6099	0.406	0.255	0.305	0.934	BS	19.4	...	1993 Jun
1738+499 ...	17 39 27.39025	49 55 03.3757	0.788	0.567	0.478	0.580	Q	17.5	1.545	1993 Mar
1742+402 ...	17 44 25.09586	40 14 48.1481	1.145	0.913	0.444	0.284	EF	–	...	1993 Jun
1745+624 ...	17 46 14.03324	62 26 54.7278	2.054	0.764	0.580	0.480	Q	18.3	3.886	1992 Sep
1746+470 ...	17 47 26.64725	46 58 50.9294	–	0.426	0.634	0.871	BS	21.3	...	1993 Mar
1747+433 ...	17 49 00.36037	43 21 51.2888	0.712	0.340	0.367	0.286	BS	17.0	...	1993 Jun
1755+578 ...	17 56 03.62851	57 48 47.9901	0.197	0.729	0.455	0.272	BS	18.0	...	1992 Sep
1806+456 ...	18 08 21.88567	45 42 20.8700	–	0.154	0.334	0.424	Q	18.6	0.830	1993 Mar
1809+568 ...	18 10 03.32027	56 49 22.9587	0.677	0.570	0.576	0.441	EF	–	...	1992 Sep
1811+430 ...	18 13 14.68906	43 04 15.6838	2.921	0.969	0.490	0.388	NS	19.4	...	1993 Mar
1812+412 ...	18 14 22.70825	41 13 05.6054	1.694	0.644	0.534	0.375	BS	18.9	...	1993 Jun
1815+614 ...	18 15 36.79199	61 27 11.6409	0.771	0.891	0.465	0.220	EF	–	...	1993 Mar
1826+796 ...	18 23 14.10905	79 38 49.0084	–	0.250	0.577	0.566	G	16.7	...	1992 Sep
1828+399 ...	18 29 56.52027	39 57 34.6902	–	0.127	0.353	0.234	EF	–	...	1993 Jun
1834+612 ...	18 35 19.67558	61 19 40.0233	1.014	0.448	0.590	0.492	BS	17.6	...	1992 Sep
1839+389 ...	18 40 57.15500	39 00 45.7119	–	–	0.476	0.221	BS	19.5[b]	...	1993 Jun
1849+670 ...	18 49 16.07136	67 05 41.6786	1.032	0.901	0.992	0.456	Q	16.0[b]	0.657	1992 Jun
1850+402 ...	18 52 30.37400	40 19 06.6006	0.554	0.546	0.535	0.616	Q	17.9[a]	2.12	1993 Jun
1851+488 ...	18 52 28.54751	48 55 47.4774	0.352	0.291	0.351	0.385	BS	18.5	...	1993 Mar
1856+737 ...	18 54 57.29825	73 51 19.9100	–	0.560	0.546	0.628	Q	15.9	0.460	1992 Sep

TABLE 1—*Continued*

Source (1)	R.A. (2)	Declination (3)	S_{80cm} (4)	S_{20cm} (5)	S_{6cm} (6)	$S_{3.6cm}$ (7)	ID (8)	*R* (9)	*z* (10)	Date (11)
1908+484 ...	19 09 46.56339	48 34 31.8265	0.620	0.575	0.423	0.244	NO	19.0[b]	...	1993 Mar
1910+375 ...	19 12 25.12308	37 40 36.6587	0.353	0.504	0.402	0.340	BS	18.5[b]	...	1993 Jun
1915+657 ...	19 15 23.81933	65 48 46.3946	0.833	0.772	0.372	0.221	RO	18.2	...	1993 Jun
1924+507 ...	19 26 06.32190	50 52 57.0209	1.423	0.656	0.354	0.434	Q	17.5[b]	1.098	1993 Jun
1936+714 ...	19 36 03.56036	71 31 31.7763	1.664	0.620	0.391	0.496	Q	18.9[b]	1.864	1992 Sep
1946+708 ...	19 45 53.51973	70 55 48.7226	0.392	0.921	0.645	0.477	G	16.7	0.101	1992 Sep
1950+573 ...	19 51 06.98368	57 27 17.1945	0.855	0.569	0.476	0.316	BS	18.0[b]	...	1992 Sep
2003+662 ...	20 03 54.51091	66 25 56.3889	1.218	1.152	0.490	0.313	EF	–	...	1992 Sep
2005+642 ...	20 06 17.69491	64 24 45.4226	–	0.174	0.739	0.973	RS	19.0[b]	...	1992 Sep
2007+659 ...	20 07 28.77132	66 07 22.5398	0.994	1.030	0.756	0.489	BS	16.4	...	1992 Jun
2015+657 ...	20 15 55.36830	65 54 52.6621	0.884	0.967	0.500	0.548	Q	19.1[a]	2.845	1992 Jun
2017+745 ...	20 17 13.07930	74 40 48.0020	–	0.472	0.500	0.341	BS	17.9	...	1992 Sep
2023+760 ...	20 22 35.58285	76 11 26.1814	–	0.383	0.426	0.374	BL	17.0[b]	–	1992 Sep
2054+611 ...	20 55 38.83705	61 22 00.6411	0.609	0.423	0.414	0.297	EF	–	...	1992 Sep
2136+824 ...	21 33 34.09726	82 39 06.0053	–	1.008	0.509	0.384	BO	18.9	...	1992 Sep
2138+389 ...	21 40 16.94765	39 11 44.8513	0.655	0.664	0.502	0.377	NS	19.0[b]	...	1993 Mar
2235+731 ...	22 36 38.60028	73 22 52.6646	–	0.300	0.424	0.346	EF	–[b]	...	1992 Sep
2238+410 ...	22 41 07.20544	41 20 11.6178	0.597	0.584	0.677	0.826	RS	17.9[b]	...	1992 Sep
2246+370 ...	22 48 37.91101	37 18 12.4680	1.251	0.906	0.414	0.307	BO	20.1	...	1992 Sep
2259+371 ...	23 01 27.73664	37 26 49.2445	0.780	0.596	0.406	0.379	BS	20.4	...	1992 Sep
2309+454 ...	23 11 47.41079	45 43 56.0250	–	0.306	0.597	0.610	EF	–	...	1993 Mar
2310+385 ...	23 12 58.79503	38 47 42.6683	0.293	0.693	0.484	0.327	Q	17.5	2.17	1993 Jun
2319+444 ...	23 22 20.35854	44 45 42.3727	0.356	0.305	0.366	0.366	NS	19.9	...	1993 Jun
2330+387 ...	23 33 02.53305	39 01 12.0185	1.252	0.844	0.394	0.357	EF	–	...	1993 Jun
2346+385 ...	23 49 20.82620	38 49 17.5725	0.259	0.322	0.640	0.286	Q	17.6	1.032	1993 Jun
2353+816 ...	23 56 22.79458	81 52 52.2669	–	0.395	0.476	0.492	BL	19.7[a]	–	1992 Sep
2356+390 ...	23 58 59.85538	39 22 28.3103	1.047	0.428	0.371	0.326	BS	20.6	...	1993 Jun
2356+385 ...	23 59 33.18089	38 50 42.3217	0.258	0.642	0.449	0.278	Q	18.6	2.704	1993 Jun

NOTES TO TABLE 1

Col. (1).—B1950 source name according to IAU convention. Cols. (2) and (3).—Right ascension and declination in J2000 coordinates from JVAS. These coordinates have an rms accuracy of ~12 milliarcsec. Cols. (4), (5), (6), and (7).—Total flux density (Jy) at wavelengths 80 cm, 20 cm, 6 cm, and 3.6 cm, from J. Douglas, private communication; White & Becker 1992; Gregory & Condon 1991; Kühr et al. 1981; JVAS. Col. (8).—Optical identification from automated scanning of the POSS plates unless otherwise noted. Key to identifications: Q—quasar; G—galaxy; BL—BL Lac object; EF—empty field; BS—blue stellar object; BO—blue object; RS—red stellar object; RO—red object; NS—neutral stellar object; NO—neutral object. Col. (9).—Apparent *R* magnitude of the object obtained by automated scanning of the POSS E plates, unless otherwise noted. The rms error is 0.3 down to magnitude 19.5 and increases to 0.5 by magnitude 20.0 (McMahon 1994). Col. (10).—Redshift; (–) indicates a featureless spectrum. Redshifts are taken from the catalog of Véron-Cetty & Véron 1993, except for the values quoted for 0651+410 from Merighi et al. 1991, 0733+597 from Stickel & Kühr 1994, 1144+352 from Morganti, Ulrich, & Tadhunter 1992, 1146+596 from Kelton 1980, and 1946+708 from Stickel & Kühr 1993. Col. (11).—Date of the VLBI observation.

Table 1 is published in computer-readable form in the AAS CD-ROM Series, Vol. 4.

[a] Identification and magnitude taken from Véron-Cetty & Véron 1993, and corrected to *R* magnitude using $\langle B - R \rangle = 0.6$.

[b] Identification and magnitude estimated by eye from the POSS plates.

[c] Identification and magnitude from Stickel & Kühr 1994.

Taylor 1994), part of the Caltech VLBI Programs. Several iterations of phase self-calibration and mapping were performed upon each source using uniform weighting, before switching to natural weighting. At each iteration, windows for clean components were added, if necessary, to provide support and reject sidelobes. Amplitude self-calibration was not performed with solution intervals smaller than 30 minutes unless the signal-to-noise ratio on all baselines was higher than ~8 (e.g., as for a compact component with flux density ≳400 mJy).

4. RESULTS

In Figure 2 we present the naturally weighted images for 91 CJ2 sources. For each image the FWHM contour of the Gaussian beam is drawn in the lower left corner and is listed in Table 3, along with the rms, peak flux density, and lowest contour level at 3 σ. The typical dynamic range in the images is 500:1. While the lowest contour may be affected by noise or small residual amplitude and phase errors, the second contour is reliable. Global fringe fitting and mapping proved difficult for three heavily resolved sources: 0733 + 597, 1436 + 763, and 2003 + 662. The north-south orientation of 0733 + 597 can be believed, but the second contour should not be trusted. The object 1436 + 763 has a flux density of 400 mJy on baselines of 5 Mλ but is undetected on baselines exceeding 50 Mλ. No naturally weighted image of 1436 + 763 at the full resolution is presented. Finally, 2003 + 662 is elongated east-west, but the second contour should not be trusted.

TABLE 2

TELESCOPE CHARACTERISTICS

Telescope (1)	Code (2)	Location (3)	Diam (m) (4)	1992 Jun (5)	1992 Sep (6)	1993 Mar (7)	T_{sys} (K) (8)	T_{sys} (Jy) (9)	Sensitivity (K/Jy) (10)
Cambridge	C	Cambridge, UK	32	√			32	140	0.23
Jodrell MKII	J2	Jodrell Bank, UK	26	√		√	44	366	0.12
Effelsberg	B	Germany	100		√	√	58	39	1.5
Onsala	S	Sweden	26	√	√	√	59	757	0.078
WSRT	W	Netherlands	5×25	√	√	√	105	133	0.86
Medicina	L	Bologna, Italy	32	√	√	√	36	225	0.16
Noto	N	Noto, Italy	32	√	√	√	35	221	0.16
Haystack	K	Westford MA, USA	36	√	√		97	606	0.16
NRAO	G	Green Bank WV, USA	43	√	√	√	34	126	0.27
VLA[a]	Y	New Mexico, USA	25	√	√	√	37	319	0.116
VLBA_BR	BR	Brewster IO, USA	25	√	√	√	37	281	0.133
VLBA_FD	FD	Fort Davis TX, USA	25	√	√		41	308	0.133
VLBA_HN	HN	Hancock NH, USA	25			√	34	259	0.133
VLBA_KP	KP	Kitt Peak AZ, USA	25	√	√	√	41	308	0.133
VLBA_LA	LA	Los Alamos NM, USA	25	√	√		38	270	0.142
VLBA_NL	NL	North Liberty IA, USA	25	√	√	√	40	300	0.133
VLBA_OV	OV	Owens Valley CA, USA	25	√	√	√	33	249	0.133
VLBA_PT	PT	Pie Town NM, USA	25	√	√	√	37	280	0.132
VLBA_SC	SC	Saint Croix VI, USA	25			√	34	255	0.133

NOTES TO TABLE 2

Cols. (1), (2), and (3).—Name, code used, and location of each telescope. Affiliations: B—Max-Planck-Institüt für Radioastronomie; O—Onsala Space Observatory; W—Westerbork Synthesis Radio Telescope, NFRA; J2, C—Nuffield Radio Astronomy Laboratories; L, N—Istituto di Radioastronomia; G—National Radio Astronomy Observatory; K—Haystack Observatory; BR, FD, HN, KP, LA, NL, OV, PT, SC—National Radio Astronomy Observatory VLBA: Y—National Radio Astronomy Observatory VLA. Col. (4).—Diameter of each telescope (in meters). Cols. (5), (6), and (7).—Tick indicates whether the telescope participated successfully in that session. Cols. (8), (9), and (10).—System temperature in K and in Jy and the sensitivity in K Jy^{-1} of each telescope. The values quoted are representative of the three sessions.

[a] The VLA was used in single-antenna mode.

Tapered images are presented in all cases where this image revealed additional information. The tapered images were produced using a Gaussian taper falling to 50% at 70 Mλ on the naturally weighted, self-calibrated data. All tapered images were restored with a circular 3 mas beam.

The rms noise in each naturally weighted image is plotted against the source declination and peak flux density in Figure 3 for all sources observed during the four sessions. There is a slight trend for higher declination sources, with correspondingly better *u-v* coverage, to have a lower noise. This result is biased, however, by the fact that many of the high-declination sources were observed during 1992 September, which had a large number of telescopes operating under favorable observing conditions. The lack of any correlation between the rms noise and the peak flux density in the map shows that the noise in the maps is predominantly limited by the thermal noise, and not by the dynamic range. The CJ2 sample is therefore an excellent, uniform sample of VLBI images.

Model fitting was performed on the self-calibrated amplitudes and phases of each source to extract quantitative information from the observations. Up to four Gaussian components were fitted to each source. The components are listed in Table 4 for all sources which produced a total agreement factor of 1.4 or better. The agreement factors are distributed as the square root of the reduced χ^2 and have an expected value of 1.0. Only two sources, 0604 + 728 and 1946 + 708, were too complex to model, and a good agreement factor could not be obtained for the heavily resolved and complex source 1436 + 763.

The average total agreement factor is 1.045. The amplitude agreement factors, presented in Table 4, are on average better by ~13% than the closure phase agreement factors. This is the result of performing the model fitting on the fully self-calibrated *u-v* data. Amplitude self-calibration at every integration period introduces N additional free parameters, where N is the number of antennas. The number of degrees of freedom is therefore reduced by a factor of approximately $(N-3)/(N-1)$ (Wieringa 1992). For 14 antennas this decreases the amplitude agreement factors by 9%.

5. SUMMARY

The CJ2 sample and its selection is described and 4992 MHz VLBI images and model fits are presented for 91 out of the 193 sources in the sample. The remaining images will be presented in Paper II (Henstock et al. 1994), along with a compilation of the integrated radio spectra. This highly uniform set of images should be well suited for morphological studies and cosmological tests. Future papers will provide interpretation of the results from the CJ2 and from statistically complete PR-CJ1-CJ2 subsamples and will present the results of a campaign to measure redshifts of the previously unobserved CJ2 sources.

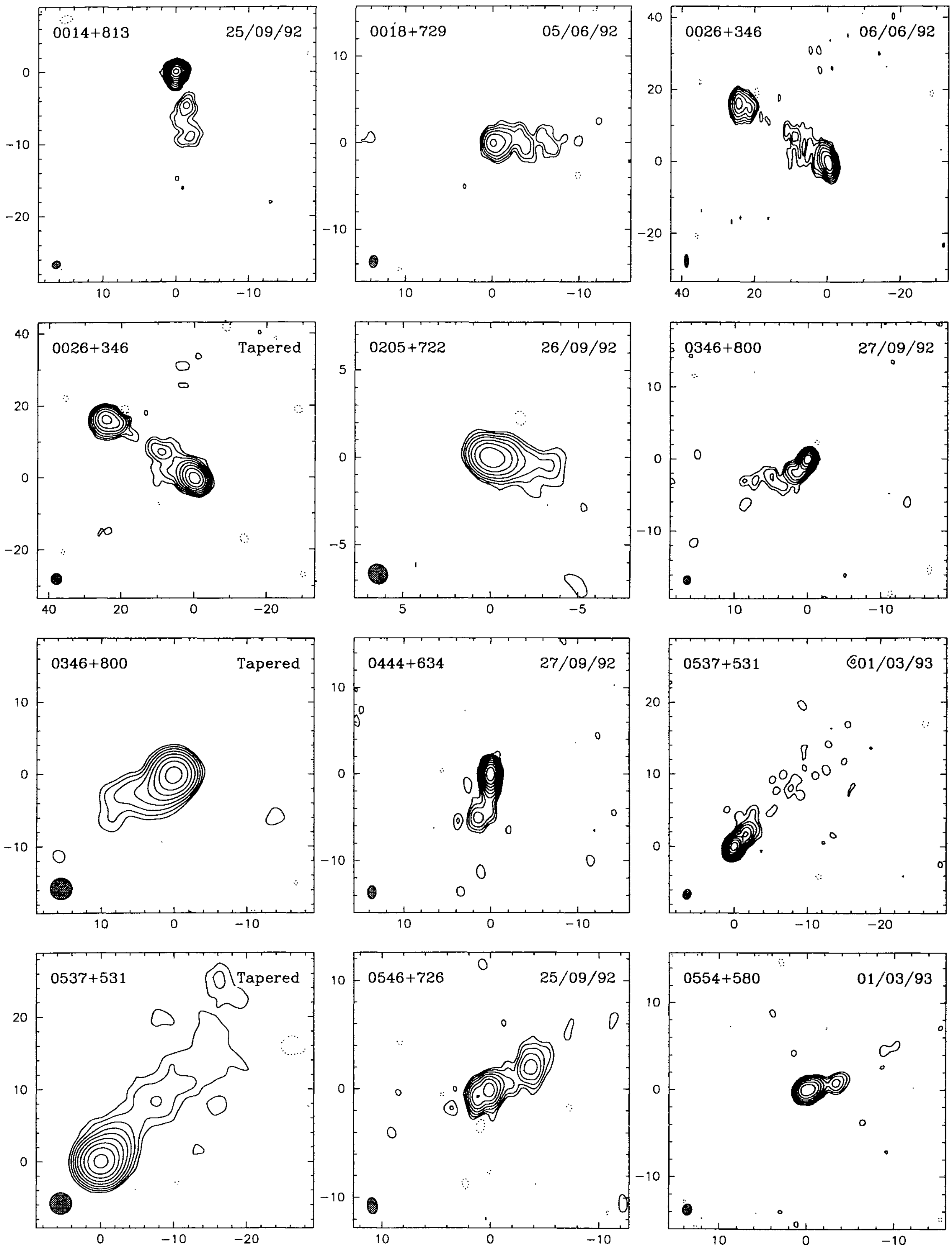

FIG. 2.—The 6 cm VLBI images for 91 sources in the CJ2 sample. Maps with the epoch of observation in the upper right corner are naturally weighted images, while those marked as "tapered" have been weighted by a Gaussian taper and restored with a 3 mas beam as described in the text. The FWHM contour of the Gaussian beam is drawn in the lower left corner and is listed in Table 3, along with the rms, peak flux density, and lowest contour level at 3 σ. Contours are drawn logarithmically at $-3\ \sigma$, $3\ \sigma$, $6\ \sigma$, $12\ \sigma$, etc., with negative contours shown as dashed lines.

FITS images corresponding to the maps presented in Fig. 2 are published in the AAS CD-ROM Series, Vol. 4.

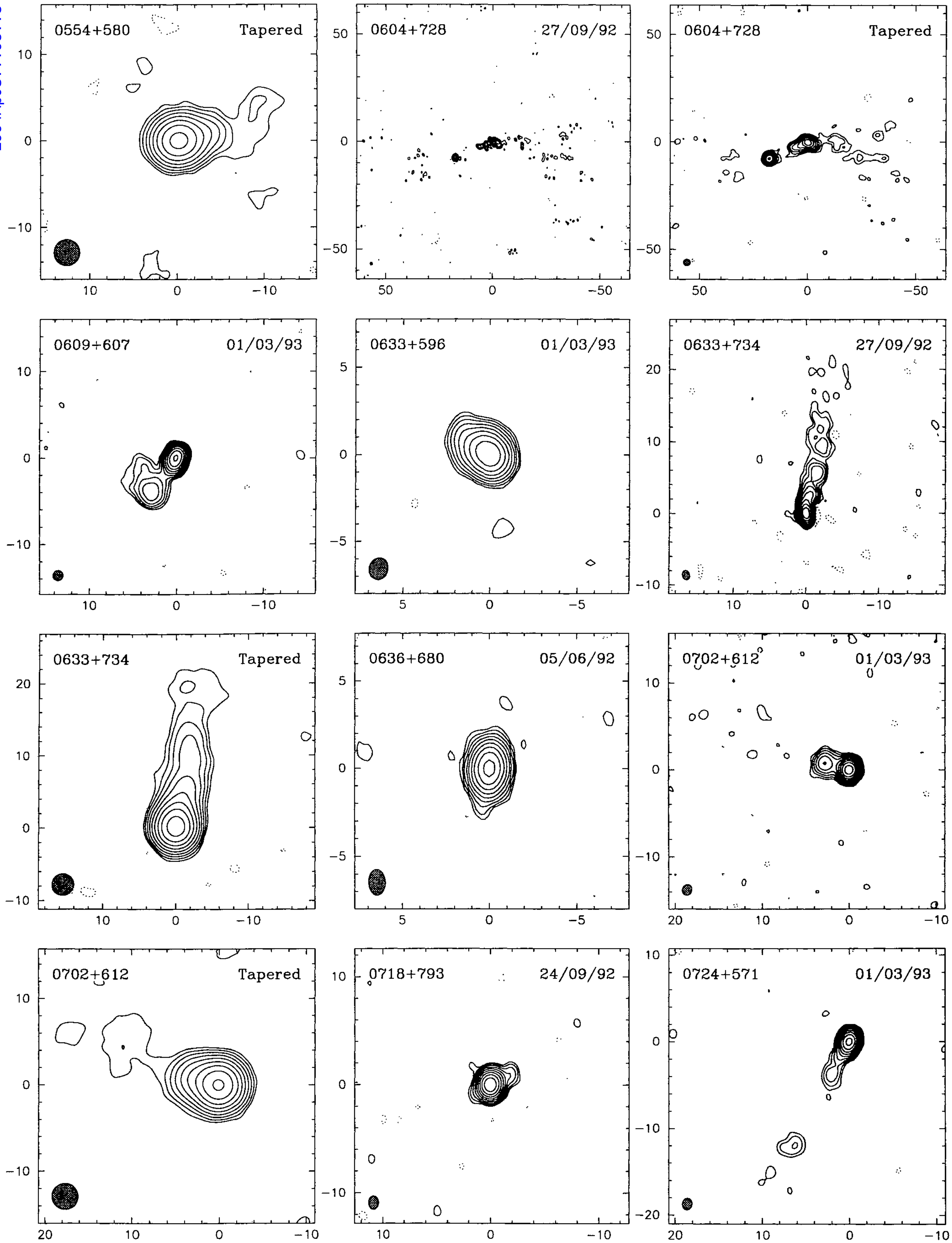

FIG. 2—*Continued*

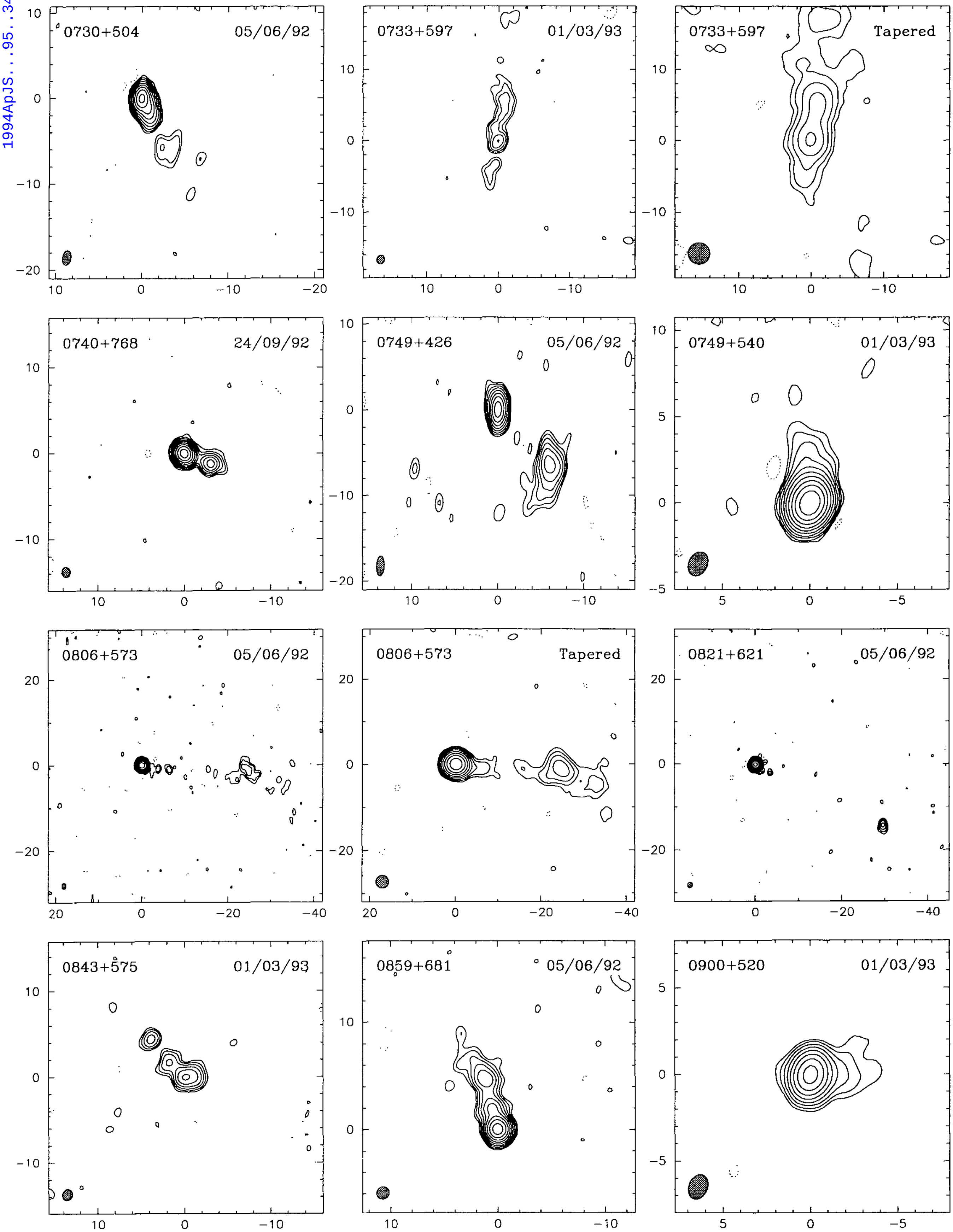

FIG. 2—*Continued*

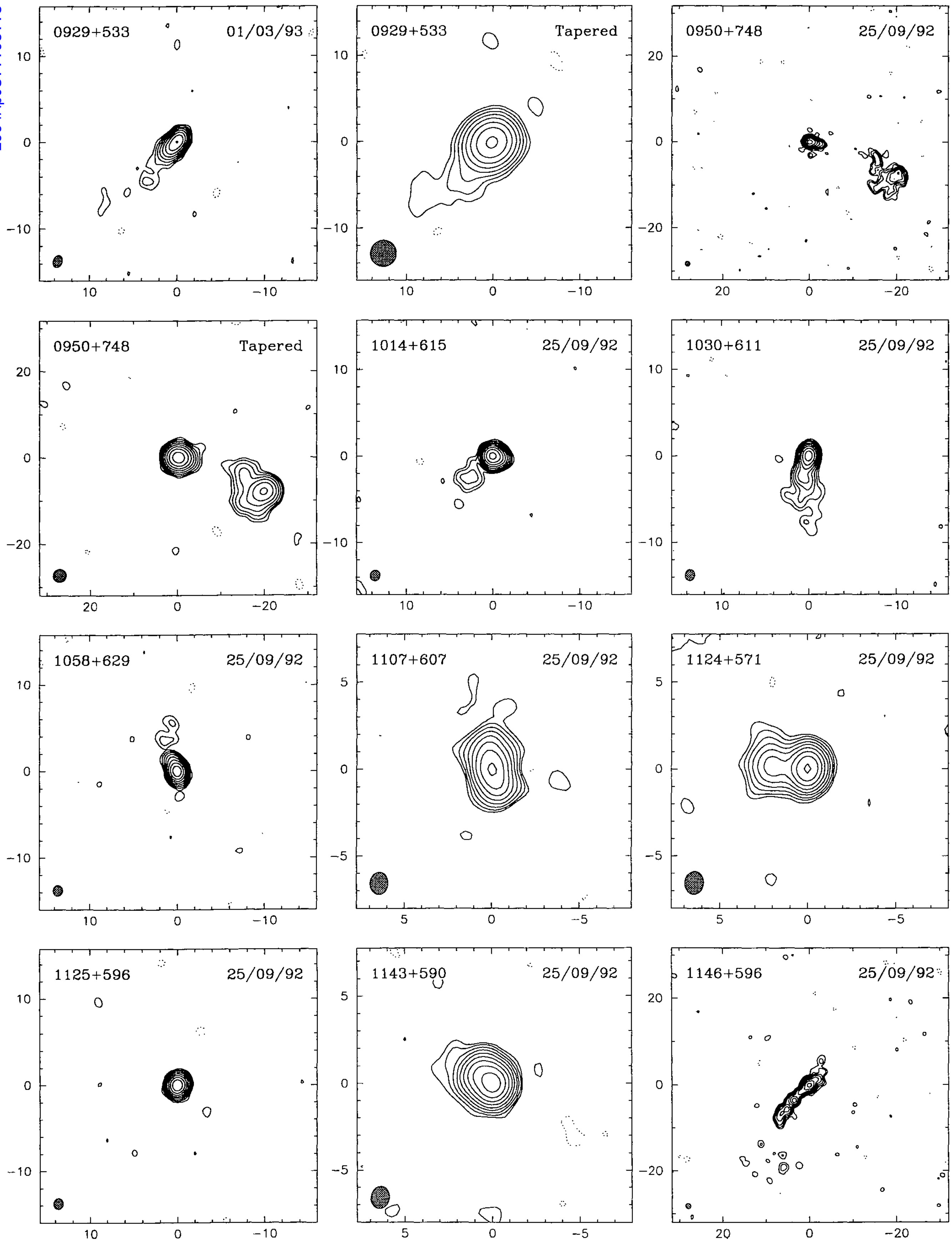

FIG. 2—*Continued*

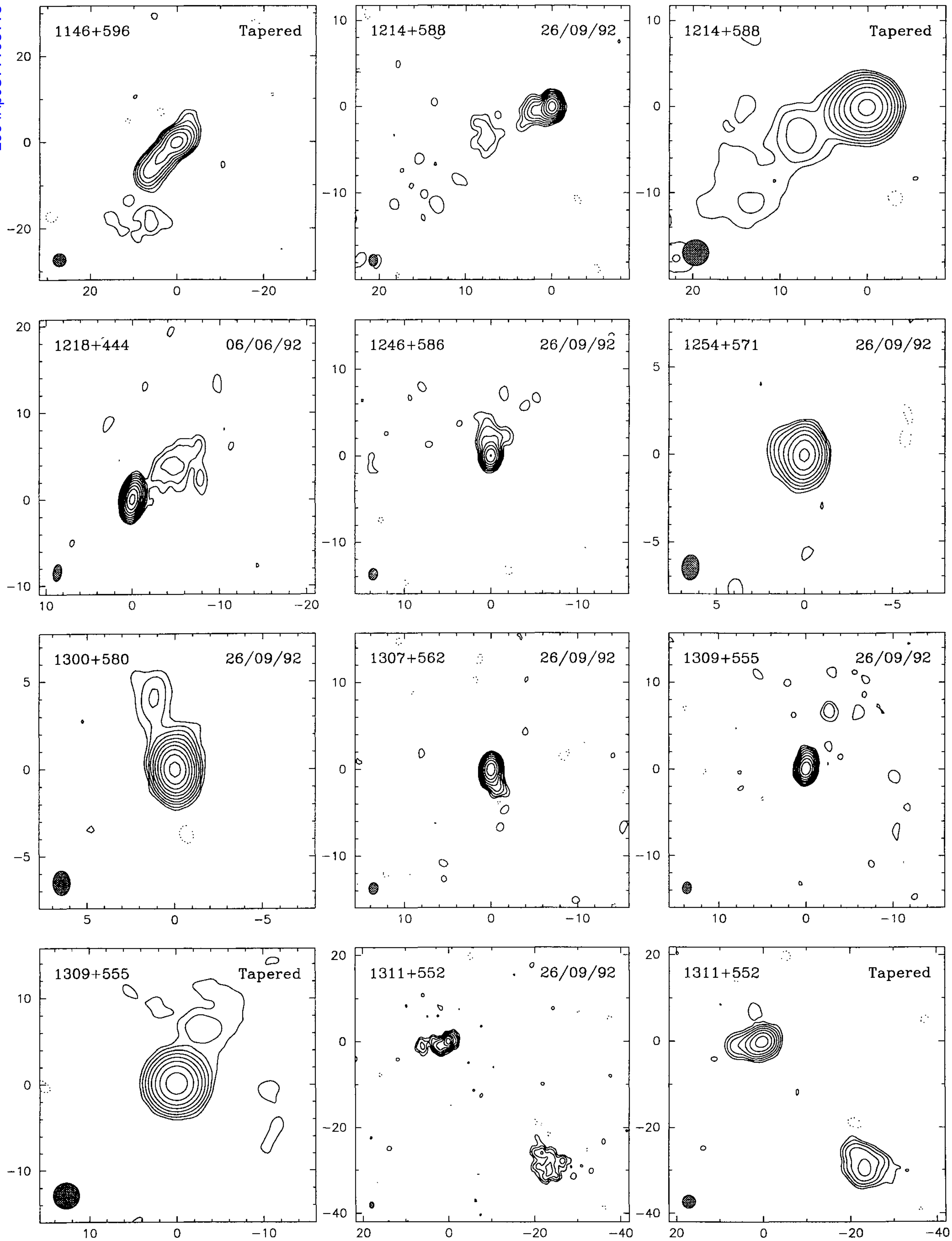

FIG. 2—*Continued*

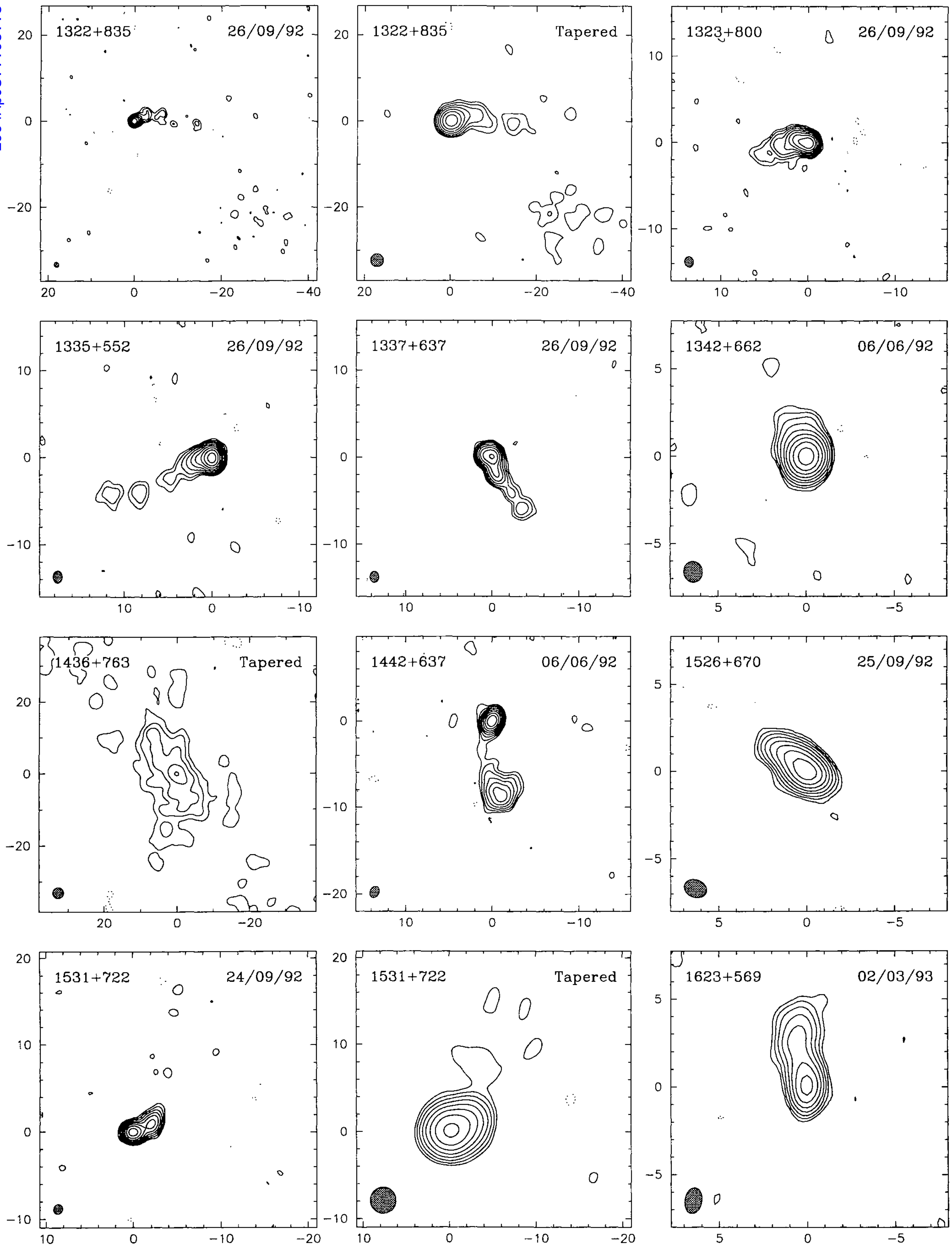

FIG. 2—*Continued*

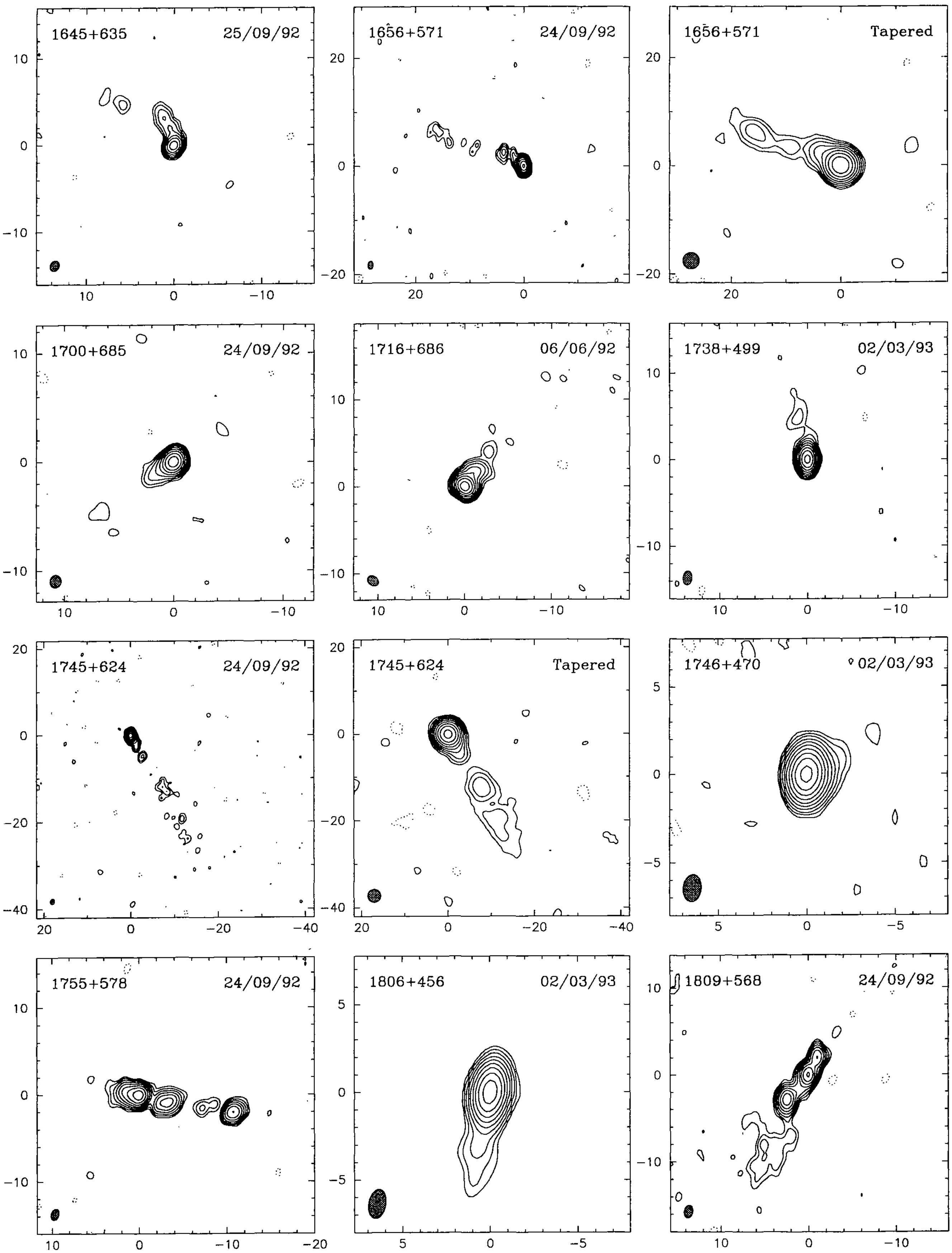

FIG. 2—*Continued*

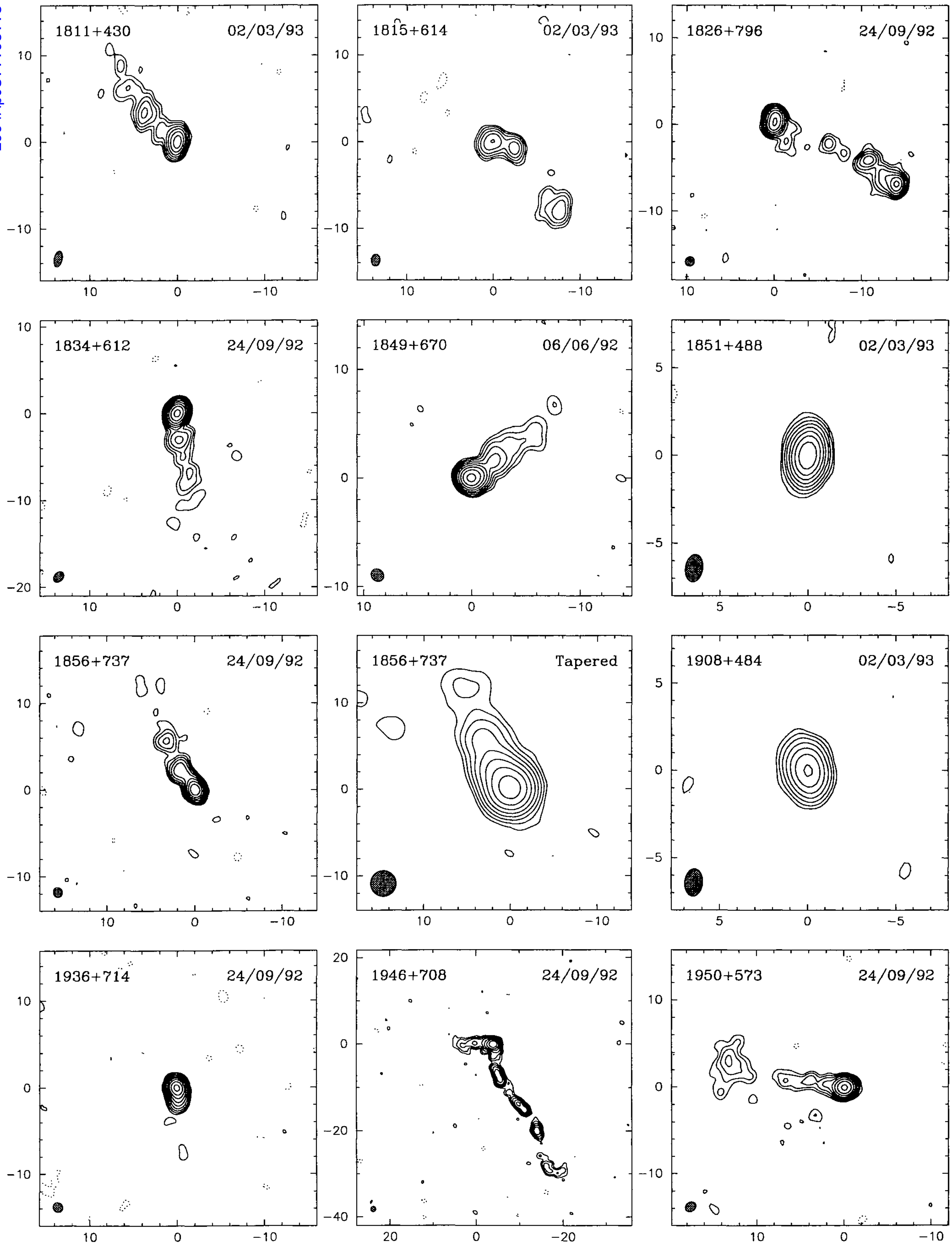

FIG. 2—*Continued*

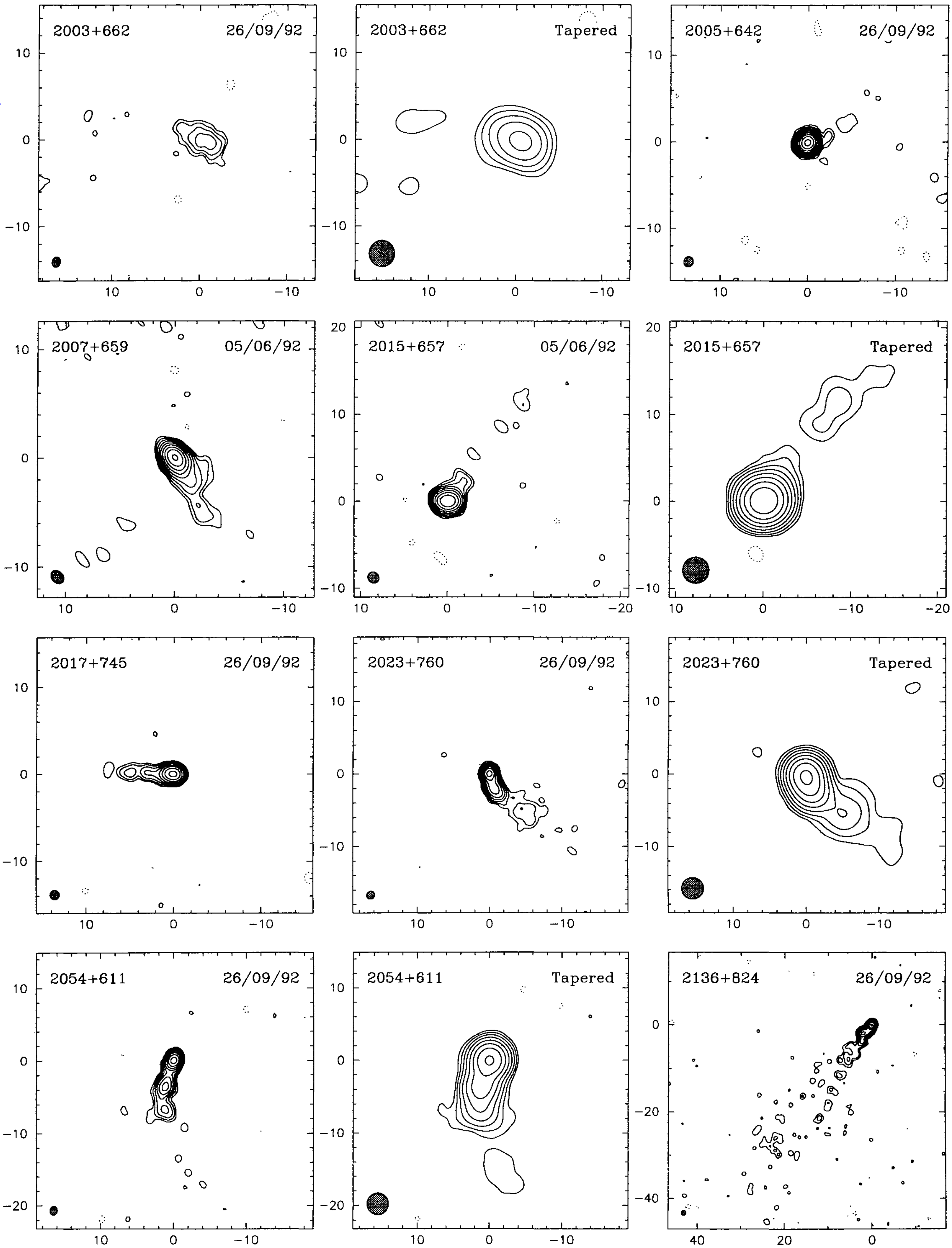

FIG. 2—*Continued*

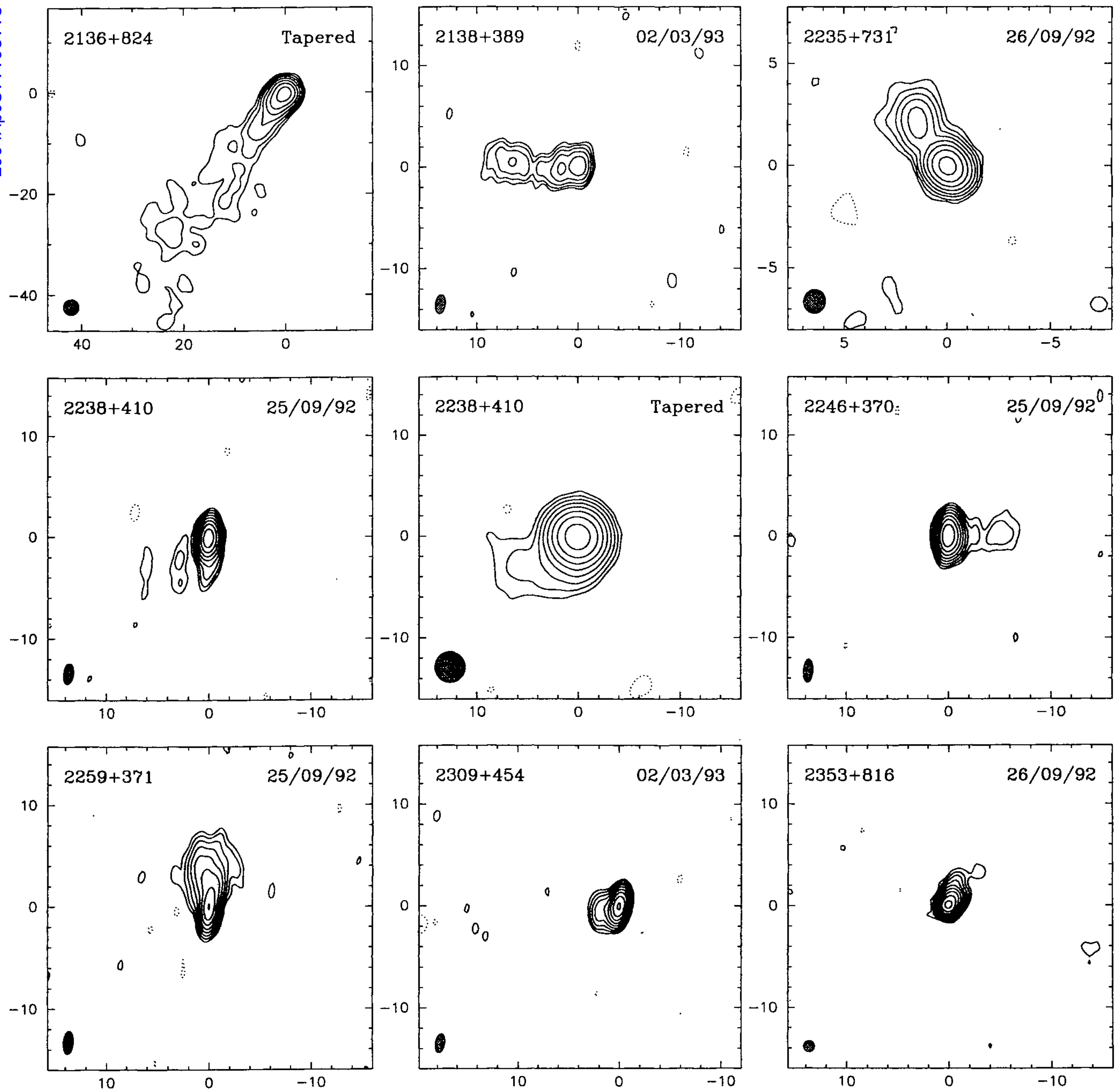

FIG. 2—*Continued*

TABLE 3

MAP PARAMETERS

Name (1)	Obs. (2)	Dur. (min) (3)	Beam a (mas) (4)	Beam b (mas) (5)	Beam θ (°) (6)	S_{nat} (mJy/beam) (7)	rms (8)	1st Cntr (%Peak) (9)	S_{tap} (mJy/beam) (10)	rms (11)	1st Cntr (%Peak) (12)
0014+813...	1992 Sep	72	1.18	1.00	−61	822	0.37	0.15			
0018+729...	1992 Jun	74	1.40	0.93	−7	64	0.58	2.70			
0026+346...	1992 Jun	73	3.64	1.00	0	269	0.72	0.80	451	0.74	0.50
0205+722...	1992 Sep	54	1.15	1.05	40	178	0.47	0.80			
0346+800...	1992 Sep	57	1.21	1.00	−7	262	0.36	0.40	305	0.54	0.55
0444+634...	1992 Sep	54	1.51	0.93	−1	548	0.37	0.20			
0537+531...	1993 Mar	60	1.41	1.05	−17	603	0.49	0.25	667	0.70	0.30
0546+726...	1992 Sep	72	1.50	0.89	7	97	0.32	1.00			
0554+580...	1993 Mar	57	1.28	1.07	−15	169	0.45	0.80	247	0.50	0.60
0604+728...	1992 Sep	54	1.35	0.94	11	93	0.44	1.40	172	0.55	0.95
0609+607...	1993 Mar	56	1.18	1.14	−30	444	0.50	0.35			
0633+596...	1993 Mar	61	1.27	1.09	−17	348	0.46	0.40			
0633+734...	1992 Sep	54	1.34	0.95	14	448	0.32	0.20	554	0.45	0.25
0636+680...	1992 Jun	59	1.47	0.96	2	399	0.40	0.30			
0702+612...	1993 Mar	57	1.27	1.10	−13	450	0.41	0.25	490	0.55	0.35
0718+793...	1992 Sep	56	1.23	0.93	−2	648	0.47	0.20			
0724+571...	1993 Mar	57	1.35	1.10	−7	454	0.43	0.30			
0730+504...	1992 Jun	54	1.70	0.97	−8	570	0.58	0.30			
0733+597...	1993 Mar	57	1.24	1.09	−16	25	0.50	6.00	44	0.80	5.45
0740+768...	1992 Sep	55	1.20	0.97	6	435	0.38	0.25			
0749+426...	1992 Jun	54	2.33	0.91	−2	244	0.39	0.50			
0749+540...	1993 Mar	57	1.46	1.05	−23	1310	0.51	0.10			
0806+573...	1992 Jun	55	1.43	1.00	0	241	0.37	0.45	331	0.49	0.45
0821+621...	1992 Jun	54	1.34	1.05	−9	425	0.41	0.30			
0843+575...	1993 Mar	57	1.35	1.17	−22	69	0.62	2.70			
0859+681...	1992 Jun	54	1.19	1.13	−43	458	0.40	0.25			
0900+520...	1993 Mar	57	1.49	1.05	−19	249	0.45	0.55			
0929+533...	1993 Mar	56	1.43	1.01	−21	159	0.40	0.75	225	0.53	0.70
0950+748...	1992 Sep	54	1.12	1.08	23	191	0.34	0.55	336	0.54	0.50
1014+615...	1992 Sep	54	1.22	1.12	−4	427	0.40	0.30			
1030+611...	1992 Sep	54	1.27	1.05	−3	258	0.42	0.50			
1058+629...	1992 Sep	54	1.23	1.06	−3	239	0.37	0.45			
1107+607...	1992 Sep	54	1.27	1.03	−4	200	0.47	0.70			
1124+571...	1992 Sep	54	1.31	1.04	−6	307	0.36	0.35			
1125+596...	1992 Sep	54	1.26	1.04	−5	274	0.37	0.40			
1143+590...	1992 Sep	54	1.27	1.06	−10	398	0.35	0.25			
1146+596...	1992 Sep	54	1.27	1.14	25	97	0.40	1.25	190	0.69	1.10
1214+588...	1992 Sep	57	1.35	1.01	0	399	0.33	0.25	443	0.43	0.30
1218+444...	1992 Jun	54	1.97	0.95	−8	429	0.43	0.30			
1246+586...	1992 Sep	54	1.35	1.02	−6	156	0.39	0.75			
1254+571...	1992 Sep	54	1.46	0.97	−4	151	0.32	0.65			
1300+580...	1992 Sep	54	1.41	0.99	0	814	0.43	0.15			
1307+562...	1992 Sep	51	1.34	1.03	−6	248	0.38	0.45			
1309+555...	1992 Sep	54	1.37	1.03	−8	253	0.36	0.45	282	0.46	0.50
1311+552...	1992 Sep	54	1.49	0.98	−1	113	0.39	1.05	194	0.68	1.05
1322+835...	1992 Sep	54	1.18	0.99	19	128	0.34	0.80	174	0.54	0.95
1323+800...	1992 Sep	54	1.22	1.00	9	268	0.38	0.45			
1335+552...	1992 Sep	54	1.40	1.00	−4	429	0.33	0.25			
1337+637...	1992 Sep	54	1.28	1.01	1	173	0.40	0.70			
1342+662...	1992 Jun	53	1.20	1.06	4	529	0.47	0.25			
1436+763...	1992 Sep	72	–	–	–	–	–	–	52	1.03	5.95
1442+637...	1992 Jun	59	1.34	1.02	−27	294	0.39	0.40			
1526+670...	1992 Sep	74	1.30	0.99	69	270	0.41	0.45			
1531+722...	1992 Sep	55	1.12	1.04	−26	216	0.37	0.50	277	0.60	0.65
1623+569...	1993 Mar	57	1.48	0.95	−10	120	0.47	1.20			

TABLE 3—*Continued*

Name	Obs.	Dur.	Beam a	Beam b	Beam θ	S_{nat}	rms	1st Cntr	S_{tap}	rms	1st Cntr
		(min)	(mas)	(mas)	(°)	(mJy/beam)		(%Peak)	(mJy/beam)		(%Peak)
(1)	(2)	(3)	(4)	(5)	(6)	(7)	(8)	(9)	(10)	(11)	(12)
1645+635...	1992 Sep	51	1.26	1.00	−33	121	0.40	1.00			
1656+571...	1992 Sep	58	1.53	0.92	−4	299	0.33	0.35	370	0.51	0.40
1700+685...	1992 Sep	55	1.18	1.03	−13	191	0.32	0.50			
1716+686...	1992 Jun	55	1.38	1.04	51	554	0.45	0.25			
1738+499...	1993 Mar	57	1.58	0.99	−4	399	0.40	0.30			
1745+624...	1992 Sep	56	1.29	0.96	−11	364	0.29	0.25	422	0.42	0.30
1746+470...	1993 Mar	56	1.55	1.02	−5	707	0.38	0.15			
1755+578...	1992 Sep	56	1.34	0.91	−19	164	0.26	0.50			
1806+456...	1993 Mar	57	1.68	0.97	−9	480	0.38	0.25			
1809+568...	1992 Sep	57	1.45	0.94	−9	167	0.40	0.70			
1811+430...	1993 Mar	56	1.85	0.93	−13	147	0.48	1.00			
1815+614...	1993 Mar	57	1.40	1.01	−4	62	0.62	3.00			
1826+796...	1992 Sep	68	1.10	1.00	−23	173	0.41	0.70			
1834+612...	1992 Sep	56	1.37	0.99	−42	377	0.38	0.30			
1849+670...	1992 Jun	54	1.26	1.09	49	454	0.42	0.30			
1851+488...	1993 Mar	57	1.59	0.97	−8	261	0.36	0.40			
1856+737...	1992 Sep	55	1.17	1.01	10	279	0.37	0.40	331	0.57	0.50
1908+484...	1993 Mar	57	1.60	1.00	−5	97	0.44	1.35			
1936+714...	1992 Sep	75	1.16	1.04	32	328	0.35	0.30			
1946+708...	1992 Sep	55	1.20	1.20	0	133	0.35	0.80			
1950+573...	1992 Sep	55	1.30	1.04	−51	181	0.39	0.65			
2003+662...	1992 Sep	54	1.19	0.96	−17	38	0.95	7.50	132	2.13	4.85
2005+642...	1992 Sep	54	1.20	1.06	−19	728	0.42	0.15			
2007+659...	1992 Jun	55	1.36	1.04	40	384	0.47	0.35			
2015+657...	1992 Jun	56	1.36	1.22	46	313	0.42	0.40	419	0.57	0.40
2017+745...	1992 Sep	54	1.11	1.08	−76	203	0.40	0.60			
2023+760...	1992 Sep	54	1.13	1.05	−25	202	0.36	0.55	272	0.59	0.65
2054+611...	1992 Sep	54	1.24	1.05	−15	198	0.37	0.55	227	0.53	0.70
2136+824...	1992 Sep	54	1.11	1.04	−6	125	0.30	0.70	159	0.52	1.00
2138+389...	1993 Mar	55	1.86	0.98	−7	54	0.65	3.60			
2235+731...	1992 Sep	53	1.15	1.04	−14	209	0.38	0.55			
2238+410...	1992 Sep	59	2.01	0.93	−6	226	0.32	0.40	272	0.43	0.45
2246+370...	1992 Sep	54	2.23	0.91	−3	270	0.34	0.40			
2259+371...	1992 Sep	54	2.26	0.91	−4	145	0.37	0.75			
2309+454...	1993 Mar	60	1.87	0.92	−10	426	0.53	0.35			
2353+816...	1992 Sep	54	1.11	1.04	−17	346	0.33	0.30			

NOTES TO TABLE 3

Col. (1).—Source name. Col. (2).—Date of observations. Col. (3).—Total integration time on source in minutes. Cols. (4), (5), and (6).—Beam characteristics of the naturally weighted maps. The restoring beam is an elliptical Gaussian with FWHM major axis a mas and minor axis b mas, with major axis in position angle θ degrees. Col. (7).—Peak flux density of the naturally weighted maps (mJy beam^{-1}). Col. (8).—Rms noise in the naturally weighted maps (mJy beam^{-1}), measured off the source in the corners of the displayed image. Col. (9).—Lowest contour level of the map in percentage of the peak flux density. Cols. (10), (11), and (12).—Peak flux density, rms noise, and lowest contour level of the tapered map, if an image has been provided. All tapered maps have been restored with a 3 mas beam.

Table 3 is published in computer-readable form in the AAS CD-ROM Series, Vol. 4.

TABLE 4

GAUSSIAN MODELS

Source	S (Jy)	r (mas)	θ (°)	a (mas)	b/a	Φ (°)	Amp. A.F.	Phase A.F.	Total A.F.
0014+813 ...	1.012	0.00	0.0	0.61	0.55	−174.3	1.067	1.291	1.175
	0.059	3.64	−165.1	4.56	0.23	21.8			
	0.023	8.32	−173.2	2.56	0.30	143.9			
0018+729 ...	0.147	0.00	0.0	0.97	0.74	10.9	1.007	1.264	1.132
	0.091	2.43	−83.4	3.30	0.69	60.6			
	0.029	6.51	−86.2	3.65	0.56	−20.3			
0026+346 ...	0.649	0.00	0.0	2.82	0.41	36.8	1.272	1.408	1.334
	0.297	29.45	56.2	2.77	0.85	27.0			
	0.100	26.73	54.1	2.61	0.33	38.6			
	0.213	4.90	50.8	11.39	0.43	55.0			
0205+722 ...	0.196	0.00	0.0	0.65	0.25	−104.4	0.921	1.078	0.996
	0.052	0.88	−102.6	0.54	0.42	−17.1			
	0.024	2.16	−103.2	1.88	0.45	−88.7			
0346+800 ...	0.304	0.00	0.0	0.56	0.45	141.7	1.001	1.087	1.041
	0.066	2.63	143.0	1.68	0.37	87.4			
	0.017	5.66	112.7	1.51	0.26	36.5			
0444+634 ...	0.607	0.00	0.0	0.61	0.38	179.2	1.019	1.045	1.031
	0.046	4.23	164.2	4.02	0.20	151.3			
0537+531 ...	0.640	0.00	0.0	0.40	0.00	−39.0	0.914	1.127	1.016
	0.107	2.27	−41.9	1.51	0.54	−33.9			
0546+726 ...	0.121	0.00	0.0	0.49	0.61	101.3	1.010	1.231	1.118
	0.075	1.22	119.3	0.66	0.00	−52.8			
	0.065	4.18	−61.4	2.64	0.43	140.5			
0554+580 ...	0.264	0.00	0.0	1.20	0.25	−80.3	1.026	1.271	1.142
	0.030	3.42	−74.2	1.06	0.75	−45.3			
0609+607 ...	0.689	0.00	0.0	1.23	0.27	161.6	0.964	1.416	1.192
	0.160	4.62	142.4	2.33	0.69	17.1			
0633+596 ...	0.328	0.00	0.0	0.69	0.39	44.8	0.889	1.084	0.983
	0.196	0.72	55.1	1.08	0.36	64.6			
0633+734 ...	0.513	0.00	0.0	0.83	0.06	−5.1	1.013	1.170	1.088
	0.138	1.79	−3.2	2.25	0.32	−21.9			
	0.081	7.23	−12.2	8.16	0.18	−6.8			
0636+680 ...	0.482	0.00	0.0	0.66	0.56	−37.3	0.908	1.034	0.968
0702+612 ...	0.481	0.00	0.0	0.41	0.37	63.9	0.915	1.061	0.984
	0.075	2.82	75.2	1.15	0.90	124.9			
0718+793 ...	0.846	0.00	0.0	0.64	0.79	86.0	0.992	1.071	1.029
0724+571 ...	0.490	0.00	0.0	0.59	0.24	151.6	0.906	1.037	0.968
	0.050	1.71	152.6	3.68	0.16	150.2			
	0.015	13.70	151.9	1.93	0.47	102.6			
0730+504 ...	0.578	0.00	0.0	0.39	0.41	28.6	0.919	1.039	0.976
	0.215	1.40	−146.8	1.23	0.42	16.2			
	0.036	6.10	−153.7	4.79	0.51	22.9			
0733+597 ...	0.048	0.00	0.0	0.76	0.74	141.3	1.039	1.287	1.157
	0.084	3.80	−9.2	11.04	0.13	−8.0			
0740+768 ...	0.559	0.00	0.0	0.66	0.76	67.7	0.913	1.033	0.970
	0.086	3.23	−111.4	0.86	0.76	84.6			

TABLE 4—*Continued*

Source	S (Jy)	r (mas)	θ (°)	a (mas)	b/a	Φ (°)	Amp. A.F.	Phase A.F.	Total A.F.
0749+426 ...	0.284	0.00	0.0	0.53	0.58	63.5	0.951	1.044	0.995
	0.140	8.92	−137.5	2.40	0.58	14.1			
0749+540 ...	1.390	0.00	0.0	0.45	0.04	56.2	0.894	1.018	0.953
	0.098	0.92	10.8	1.07	0.75	−20.8			
0806+573 ...	0.354	0.00	0.0	0.96	0.37	86.8	1.037	1.171	1.101
	0.046	24.61	−92.8	3.89	0.80	54.4			
0821+621 ...	0.562	0.00	0.0	0.86	0.00	73.2	0.953	1.007	0.978
	0.021	32.74	−115.8	0.90	0.62	179.1			
0843+575 ...	0.143	0.00	0.0	1.54	0.56	−83.8	1.121	1.333	1.215
	0.028	2.52	49.1	1.08	0.00	6.2			
	0.025	6.01	41.7	0.48	0.50	169.4			
0859+681 ...	0.478	0.00	0.0	0.48	0.20	21.1	0.931	1.033	0.980
	0.123	1.52	12.6	1.99	0.51	26.4			
	0.073	4.94	14.1	1.82	0.47	47.7			
0900+520 ...	0.285	0.00	0.0	0.57	0.46	49.6	1.000	1.004	1.002
	0.017	1.51	−95.9	1.25	0.69	−2.6			
0929+533 ...	0.164	0.00	0.0	0.67	0.31	129.8	1.043	1.138	1.087
	0.091	1.08	137.5	0.81	0.67	90.4			
	0.015	5.11	144.7	4.83	0.14	119.2			
0950+748 ...	0.308	0.00	0.0	0.96	0.90	−77.6	1.031	1.256	1.140
	0.091	1.22	−92.8	1.22	0.62	14.2			
	0.027	16.37	−104.2	2.50	0.00	25.8			
	0.237	21.17	−112.6	3.99	0.57	−57.1			
1014+615 ...	0.468	0.00	0.0	0.51	0.78	47.8	0.883	1.025	0.951
	0.093	0.93	−105.5	0.58	0.00	−129.0			
	0.029	3.54	135.3	2.66	0.56	111.2			
1030+611 ...	0.321	0.00	0.0	0.74	0.50	165.0	1.079	1.148	1.112
	0.057	2.79	166.0	1.41	0.87	165.6			
1058+629 ...	0.224	0.00	0.0	0.27	0.69	11.8	0.910	1.052	0.978
	0.071	0.80	27.1	0.94	0.00	19.1			
	0.012	3.68	15.0	2.10	0.19	111.7			
1107+607 ...	0.389	0.00	0.0	1.43	0.50	18.3	1.133	1.228	1.177
1124+571 ...	0.321	0.00	0.0	0.36	0.83	72.5	0.962	1.022	0.990
	0.103	1.88	88.1	1.31	0.69	55.9			
1125+596 ...	0.330	0.00	0.0	0.59	0.68	88.4	0.863	1.026	0.941
1143+590 ...	0.438	0.00	0.0	0.51	0.70	66.5	0.889	1.023	0.953
	0.143	0.96	55.9	0.42	0.54	145.0			
1146+596 ...	0.187	0.00	0.0	1.38	0.74	43.5	1.204	1.331	1.263
	0.055	4.92	135.9	0.45	0.00	113.6			
	0.259	5.35	134.8	11.99	0.09	138.0			
1214+588 ...	0.395	0.00	0.0	0.31	0.00	119.6	0.891	1.012	0.948
	0.089	1.23	114.0	2.40	0.28	94.5			
	0.020	8.41	113.2	3.82	0.68	−4.0			
1218+444 ...	0.467	0.00	0.0	0.50	0.47	134.9	0.935	1.041	0.986
	0.074	4.93	−50.2	8.22	0.32	120.4			

TABLE 4—*Continued*

Source	S (Jy)	r (mas)	θ (°)	a (mas)	b/a	Φ (°)	Amp. A.F.	Phase A.F.	Total A.F.
1246+586 ...	0.177	0.00	0.0	0.56	0.67	178.7	0.942	1.051	0.993
	0.038	2.09	0.1	2.18	0.59	−6.9			
1254+571 ...	0.188	0.00	0.0	0.58	0.87	92.4	0.940	1.058	0.996
1300+580 ...	0.881	0.00	0.0	0.44	0.48	42.0	0.912	1.008	0.957
	0.022	2.93	18.9	2.04	0.59	19.3			
1307+562 ...	0.272	0.00	0.0	0.59	0.50	−2.7	0.940	1.008	0.972
	0.051	1.04	−178.1	0.10	0.72	−150.2			
1309+555 ...	0.292	0.00	0.0	0.71	0.23	−12.3	1.043	1.081	1.061
1311+552 ...	0.148	0.00	0.0	0.93	0.74	15.1	0.940	1.186	1.058
	0.142	1.86	120.2	2.76	0.59	103.0			
	0.152	36.87	−141.7	5.96	0.66	−157.1			
	0.019	6.39	103.1	2.12	0.37	137.5			
1322+835 ...	0.181	0.00	0.0	0.80	0.51	−63.6	1.052	1.145	1.095
	0.032	2.91	−76.3	1.37	0.44	3.6			
1323+800 ...	0.313	0.00	0.0	0.65	0.39	93.3	0.929	1.047	0.985
	0.162	1.23	75.6	0.86	0.69	54.3			
	0.068	2.91	97.1	2.35	0.83	123.8			
1335+552 ...	0.500	0.00	0.0	0.62	0.47	76.8	0.910	1.008	0.956
	0.095	1.37	96.4	1.18	0.56	103.4			
	0.032	8.56	113.1	9.05	0.13	104.2			
1337+637 ...	0.236	0.00	0.0	1.15	0.00	77.5	1.044	1.187	1.112
	0.106	1.34	−168.8	1.44	0.00	−173.6			
	0.031	4.53	−150.5	0.85	0.00	−16.9			
	0.016	7.16	−150.8	1.10	0.35	111.8			
1342+662 ...	0.609	0.00	0.0	0.48	0.76	−28.5	0.893	1.024	0.955
1442+637 ...	0.318	0.00	0.0	0.33	0.84	−14.6	0.975	1.051	1.011
	0.184	8.44	−173.5	2.08	0.85	48.2			
1526+670 ...	0.239	0.00	0.0	0.52	0.22	70.4	0.919	1.030	0.971
	0.175	1.02	39.7	1.20	0.17	56.1			
1531+722 ...	0.262	0.00	0.0	0.67	0.43	−80.9	0.915	1.064	0.986
	0.090	2.39	−63.6	1.30	0.55	−36.4			
1623+569 ...	0.118	0.00	0.0	0.59	0.41	11.2	1.029	1.090	1.057
	0.107	1.74	12.6	3.24	0.18	11.1			
1645+635 ...	0.133	0.00	0.0	0.39	0.64	7.2	0.991	1.086	1.036
	0.039	2.35	15.1	3.48	0.18	29.5			
	0.006	7.42	49.8	1.08	0.00	19.0			
1656+571 ...	0.377	0.00	0.0	0.74	0.49	41.0	0.981	1.067	1.021
	0.020	3.01	42.2	0.53	0.00	133.9			
	0.021	4.59	56.5	0.75	0.77	133.8			
1700+685 ...	0.191	0.00	0.0	0.27	0.11	148.5	0.984	1.025	1.003
	0.035	0.83	124.1	0.68	0.74	125.5			
1716+686 ...	0.638	0.00	0.0	0.64	0.00	150.3	0.894	1.043	0.965
	0.106	1.61	−31.0	1.89	0.26	133.3			
	0.007	5.39	−32.0	1.11	0.01	48.6			
1738+499 ...	0.464	0.00	0.0	0.65	0.55	21.2	0.907	1.020	0.960

TABLE 4—*Continued*

Source	S (Jy)	r (mas)	θ (°)	a (mas)	b/a	Φ (°)	Amp. A.F.	Phase A.F.	Total A.F.
1745+624 ...	0.421	0.00	0.0	0.60	0.46	−155.9	0.988	1.065	1.024
	0.037	2.52	−151.8	1.99	0.25	3.1			
	0.014	5.24	−155.2	0.81	0.58	−66.8			
1746+470 ...	0.756	0.00	0.0	0.33	0.94	94.0	0.937	1.043	0.987
1755+578 ...	0.240	0.00	0.0	0.86	0.43	67.1	0.992	1.131	1.058
	0.094	3.31	−104.6	1.78	0.36	−81.8			
	0.081	10.96	−100.7	0.96	0.00	−98.9			
	0.065	1.19	79.0	0.96	0.25	50.5			
1806+456 ...	0.492	0.00	0.0	0.35	0.39	172.9	0.875	1.001	0.935
	0.020	1.63	173.6	1.34	0.49	163.2			
1809+568 ...	0.196	0.00	0.0	0.56	0.71	27.7	1.157	1.242	1.197
	0.177	3.67	139.4	0.74	0.88	−15.5			
	0.101	2.29	−25.7	0.59	0.65	−5.8			
1811+430 ...	0.183	0.00	0.0	0.63	0.17	60.9	1.058	1.113	1.083
	0.015	1.35	54.7	1.50	0.39	21.2			
	0.060	5.02	47.5	2.06	0.44	−5.4			
	0.015	8.51	41.6	1.69	0.00	104.4			
1815+614 ...	0.182	0.00	0.0	1.07	0.83	−104.3	1.174	1.577	1.366
	0.033	3.27	−101.0	1.35	0.40	−32.5			
	0.092	10.09	−138.2	3.08	0.74	−118.1			
1826+796 ...	0.358	0.00	0.0	1.43	0.42	−11.8	1.416	1.608	1.507
	0.013	6.74	−104.3	0.00	0.16	−44.8			
	0.070	11.61	−110.9	0.93	0.36	−111.4			
	0.156	15.61	−116.4	1.04	0.51	−171.2			
1834+612 ...	0.466	0.00	0.0	0.78	0.25	−166.4	0.894	1.023	0.955
	0.046	2.92	−176.9	1.15	0.57	−117.8			
	0.040	7.48	−171.2	7.81	0.23	−176.9			
1849+670 ...	0.564	0.00	0.0	0.75	0.36	120.4	0.932	1.098	1.012
	0.075	2.75	−50.3	0.97	0.74	179.4			
	0.028	6.15	−51.9	3.50	0.34	−34.2			
1851+488 ...	0.273	0.00	0.0	0.31	0.73	38.4	0.990	1.008	0.998
1856+737 ...	0.291	0.00	0.0	0.49	0.00	23.6	0.959	1.036	0.995
	0.097	1.82	35.0	2.78	0.24	47.7			
	0.047	5.51	27.4	5.80	0.27	26.3			
1908+484 ...	0.145	0.00	0.0	0.97	0.64	42.6	0.853	1.170	1.007
1936+714 ...	0.284	0.00	0.0	0.28	0.00	39.4	0.905	1.041	0.970
	0.138	0.71	−166.1	1.45	0.24	0.6			
1950+573 ...	0.220	0.00	0.0	0.75	0.14	53.6	0.870	1.086	0.975
	0.053	2.58	82.2	6.04	0.12	83.7			
	0.050	13.23	78.4	3.23	0.71	19.5			
2003+662 ...	0.150	0.00	0.0	3.65	0.71	55.8	1.391	1.332	1.364
	0.100	1.58	−113.9	1.09	0.81	2.3			
2005+642 ...	0.802	0.00	0.0	0.43	0.64	−81.2	0.929	1.021	0.973
2007+659 ...	0.482	0.00	0.0	0.74	0.55	29.4	0.965	1.104	1.031
	0.045	2.65	−149.9	1.00	0.30	−38.6			
2015+657 ...	0.439	0.00	0.0	1.17	0.32	97.8	1.001	1.036	1.017
	0.028	1.59	−45.7	2.56	0.33	−33.7			

TABLE 4—*Continued*

Source	S (Jy)	r (mas)	θ (°)	a (mas)	b/a	Φ (°)	Amp. A.F.	Phase A.F.	Total A.F.
2017+745 ...	0.275	0.00	0.0	0.92	0.21	81.9	1.025	1.100	1.060
	0.037	2.83	85.4	3.12	0.00	80.2			
2023+760 ...	0.217	0.00	0.0	0.51	0.00	28.7	0.908	1.010	0.956
	0.152	2.01	−162.1	1.84	0.38	29.5			
	0.043	7.29	−135.4	5.78	0.60	−116.1			
2054+611 ...	0.228	0.00	0.0	0.56	0.42	148.3	0.910	1.037	0.971
	0.100	3.69	162.7	1.64	0.49	160.5			
	0.032	7.03	169.6	2.02	0.61	−134.0			
2136+824 ...	0.150	0.00	0.0	0.53	0.53	142.1	1.076	1.102	1.088
	0.064	2.75	134.8	1.08	0.52	111.5			
	0.070	8.08	147.7	19.93	0.10	149.6			
2138+389 ...	0.080	0.00	0.0	0.92	0.82	30.1	1.010	1.307	1.147
	0.163	3.54	91.4	7.25	0.23	87.0			
2235+731 ...	0.262	0.00	0.0	0.81	0.10	48.3	0.898	1.029	0.960
	0.058	2.54	35.0	1.66	0.40	19.3			
2238+410 ...	0.293	0.00	0.0	0.73	0.82	24.1	0.949	1.046	0.995
2246+370 ...	0.369	0.00	0.0	0.81	0.75	−95.1	1.060	1.058	1.059
	0.018	2.14	−85.2	2.56	0.20	−77.2			
2259+371 ...	0.192	0.00	0.0	1.20	0.40	168.4	0.910	1.095	0.999
	0.149	3.01	−1.0	2.92	0.57	42.2			
2309+454 ...	0.431	0.00	0.0	0.42	0.00	135.2	0.915	1.274	1.091
	0.072	1.07	116.4	2.23	0.13	93.8			
2353+816 ...	0.310	0.00	0.0	0.29	0.84	141.0	0.924	1.035	0.977
	0.174	0.85	−27.0	0.99	0.62	−32.2			

NOTES TO TABLE 4

Table reports parameters of each Gaussian component of the model brightness distribution: S, flux density; r, θ, polar coordinates of the center of the component relative to an arbitrary origin, with polar angle measured from north through east; a, b, major and minor axes of the FWHM contour; Φ, position angle of the major axis measured from north through east. The sources 0604+728, 1436+763, and 1946+708 were too complicated to model.

Table 4 is published in computer-readable form in the AAS CD-ROM Series, Vol. 4.

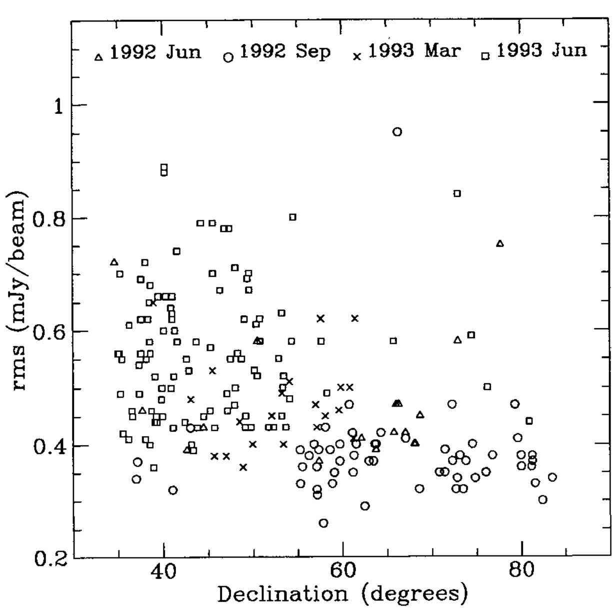

FIG. 3*a*

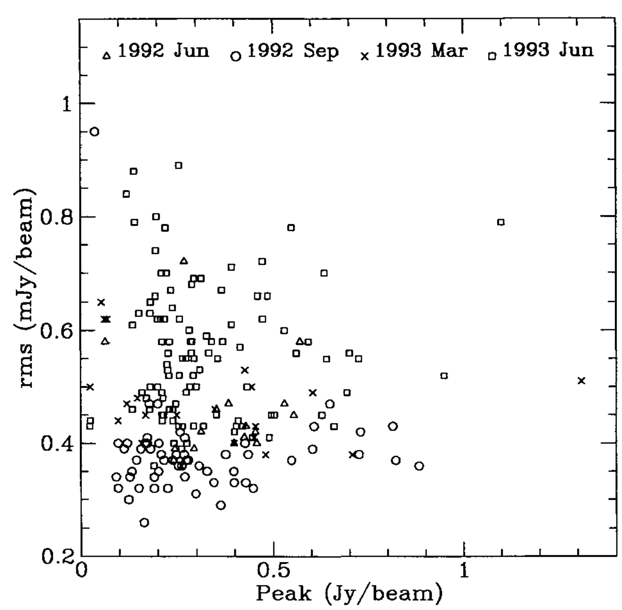

FIG. 3*b*

FIG. 3.—Rms noise from the naturally weighted maps is plotted (*a*) against the source declination and (*b*) against the peak in the map for all sources mapped during the four observing sessions, including the 1993 June session described in Paper II.

We thank the staffs at the observatories that took part in these observations and the staff of the JPL/Caltech Block II Correlator for their assistance. We thank R. McMahon for undertaking the APM scanning of the POSS plates and J. Douglas for supplying 365 MHz flux densities prior to publication. We also thank M. Shepherd for writing DIFMAP and for the many modifications he made on our behalf. The work done by the Caltech group was supported by NSF grant AST-9117100. D. R. H. gratefully acknowledges the receipt of a SERC research studentship. This research has made use of the NASA/IPAC Extragalactic Database (NED), which is operated by the Jet Propulsion Laboratory, Caltech, under contract with the National Aeronautics and Space Administration.

REFERENCES

Condon, J. J., & Broderick, J. J. 1985, AJ, 90, 2540
———. 1986, AJ, 91, 1051
Condon, J. J., Broderick, J. J., & Seielstad, G. A. 1989, AJ, 97, 1064
Gregory, P. C., & Condon, J. J. 1991, ApJS, 75, 1011
Henstock, D. R. 1994, Ph.D. thesis, Univ. Manchester
Henstock, D. R., Browne, I. W. A., Wilkinson, P. N., Taylor, G. B., Vermeulen, R. C., Pearson, T. J., & Readhead, A. C. S. 1994, ApJS, in preparation (Paper II)
Kelton, P. W. 1980, AJ, 85, 89
Kühr, H., Pauliny-Toth, I. I. K., Witzel, A., & Schmidt, J. 1981, AJ, 86, 854
McMahon, R. G. 1994, in preparation
Merighi, R., Basso, L., Vigotti, M., Lahulla, J. F., & Lopez-Arroyo, M. 1991, A&AS, 89, 225
Morganti, R., Ulrich, M.-H., & Tadhunter, C. N. 1992, MNRAS, 254, 546
Patnaik, A. R., Browne, I. W. A., Wilkinson, P. N., & Wrobel, J. M. 1992, MNRAS, 254, 655 (JVAS)
Pearson, T. J., & Readhead, A. C. S. 1988, ApJ, 328, 114 (PR)
Polatidis, A. G., Wilkinson, P. N., Xu, W., Readhead, A. C. S., Pearson, T. J., Taylor, G. B., & Vermeulen, R. C. 1994, ApJS, in press
Schwab, F. R. & Cotton, W. D. 1983, AJ, 88, 688
Shepherd, M. C., Pearson, T. J., & Taylor, G. B. 1994, BAAS, 26, 987
Stickel, M., & Kühr, H. 1993, A&AS, 100, 395
———. 1994, A&AS, 103, 349
Taylor, G. B., Vermeulen, R. C., Pearson, T. J., Readhead, A. C. S., Henstock, D. R., Browne, I. W. A., & Wilkinson, P. N. 1994, ApJ, in preparation
Thakkar, D. D., Xu, W., Readhead, A. C. S., Pearson, T. J., Taylor, G. B., Vermeulen, R. C., Polatidis, A. G., & Wilkinson, P. N. 1994, ApJS, in press
Véron-Cetty, M.-P., & Véron, P. 1993, ESO Sci Rep. No. 13
White, R. L., & Becker, R. H. 1992, ApJS, 79, 331
Wieringa, M. H. 1992, Exp. Astron., 2, 203
Xu, W. 1994, Ph.D. thesis, Caltech